Journal of proteome research

pubs.acs.org/jpr

Article

Rabbit Antidiethoxyphosphotyrosine Antibody, Made by Single B Cell Cloning, Detects Chlorpyrifos Oxon-Modified Proteins in Cultured Cells and Immunopurifies Modified Peptides for Mass Spectrometry

Seda Onder, Marco van Grol, Alex Fidder, Gaoping Xiao, Daan Noort, Udaya Yerramalla, Ozden Tacal, Lawrence M. Schopfer, and Oksana Lockridge*

Cite This: *J. Proteome Res.* 2021, 20, 4728–4745

Read Online

ACCESS | Metrics & More | Article Recommendations | Supporting Information

ABSTRACT: Chronic low-dose exposure to organophosphorus pesticides is associated with the risk of neurodegenerative disease. The mechanism of neurotoxicity is independent of acetylcholinesterase inhibition. Adducts on tyrosine, lysine, threonine, and serine can occur after exposure to organophosphorus pesticides, the most stable being adducts on tyrosine. Rabbit monoclonal 1C6 to diethoxyphosphate-modified tyrosine (depY) was created by single B cell cloning. The amino acid sequence and binding constant (K_d 3.2 × 10^{-8} M) were determined. Cultured human neuroblastoma SH-SY5Y and mouse neuroblastoma N2a cells incubated with a subcytotoxic dose of 10 μM chlorpyrifos oxon contained depY-modified proteins detected by monoclonal 1C6 on Western blots. depY-labeled peptides from tryptic digests of cell lysates were immunopurified by binding to immobilized 1C6. Peptides released with 50% acetonitrile and 1% formic acid were analyzed by liquid chromatography tandem mass spectrometry (LC-MS/MS) on an Orbitrap Fusion Lumos mass spectrometer. Protein Prospector database searches identified 51 peptides modified on tyrosine by diethoxyphosphate in SH-SY5Y cell lysate and 73 diethoxyphosphate-modified peptides in N2a cell lysate. Adducts appeared most frequently on the cytoskeleton proteins tubulin, actin, and vimentin. It was concluded that rabbit monoclonal 1C6 can be useful for studies that aim to understand the mechanism of neurotoxicity resulting from low-dose exposure to organophosphorus pesticides.

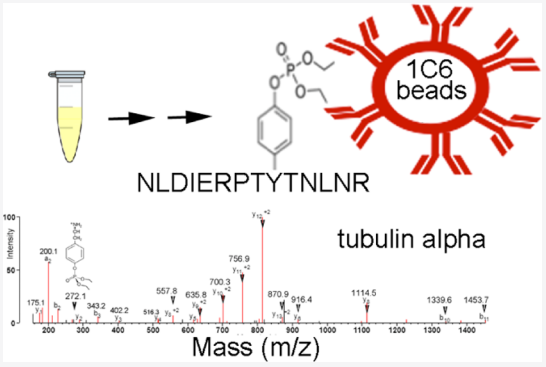

KEYWORDS: *diethoxyphosphotyrosine, mass spectrometry, Protein Prospector, N2a neuroblastoma, SH-SY5Y, single B cell cloning, rabbit monoclonal*

INTRODUCTION

The mechanism by which organophosphorus pesticides (OPs) and nerve agents cause acute toxicity is understood.[1] Thousands of publications have confirmed that these chemicals inhibit the activity of acetylcholinesterase (AChE). The inhibited acetylcholinesterase (AChE) cannot perform its function of hydrolyzing the neurotransmitter acetylcholine at cholinergic synapses. Acute symptoms of AChE inhibition include impaired breathing and death.

The involvement of targets other than AChE to explain toxicity due to exposure to OP has been proposed based on observations in animals and humans. Rats treated with a variety of organophosphates at doses that produce the same level of AChE inhibition display different signs of toxicity.[2] Humans exposed to sarin in the Tokyo subway attack in 1995 continued to have problems with blurred vision, fatigue, lethargy, forgetfulness, insomnia, and post-traumatic stress 10 years after the event.[3] The risk of neurodegenerative disease is associated with chronic exposure to OP at doses too low to inhibit AChE.[4−6]

The present report describes a rabbit monoclonal antibody that recognizes diethoxyphospho adducts on tyrosine in proteins. The antibody detects modified proteins on Western blots and immunopurifies diethoxyphosphotyrosine (depY)-modified peptides. Mass spectrometry analysis of the immunopurified peptides from human SH-SY5Y neuroblastoma cells treated with 10 μM chlorpyrifos oxon (CPO) identified 51 modified peptides. Similar treatment of mouse N2a neuroblastoma cells identified 73 modified peptides. This

Received: May 11, 2021
Published: September 1, 2021

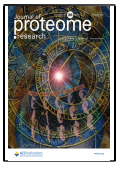

work provides a new tool for studying the mechanism of neurotoxicity associated with exposure to low doses of OP.

MATERIALS

The materials used were as follows: Keyhole limpet hemocyanin *Megathura crenulata* (Calbiochem #374805), trypsin sequencing grade (Promega #V5113), rabbit anti-diethoxyphosphotyrosine monoclonal 1C6 (present report), mouse antidiethoxyphosphotyrosine monoclonal 3B9,[7] mouse anti β actin (Thermo Fisher AM4302), antirabbit immunoglobulin G-horseradish peroxidase (IgG-HRP) (Cell Signaling #70745), antimouse IgG-HRP (Cell Signaling #7076S), Halt protease inhibitor cocktail (Thermo Scientific #87786), purified human butyrylcholinesterase prepared in-house,[8] 1-ethyl-3-[3-dimethylaminopropyl]carbodiimide hydrochloride (EDC) (Fluka #03450), chlorpyrifos oxon (Chem Service MET-11459B), dichlorvos (Chem Service N-11675), *trans*-retinoic acid (Sigma-Aldrich 554720), CNBr-activated Sepharose 4B (Amersham Biosciences AB #17-981-01), Opti-MEM (Gibco 31985-070), Dulbecco's modified Eagle's medium (DMEM)/F12 (Glutamax Gibco 10565-018), radioimmunoprecipitation assay (RIPA) buffer (Pierce #89900), immunoprecipitation (IP) lysis buffer (Pierce 87787 Thermo Fisher Scientific), Clarity Max Western ECL Substrate (Bio-Rad #1705062), Super Signal West Femto maximum sensitivity substrate (Pierce #34095), ECL Super Signal West Dura Substrate Trial Kit (Thermo Scientific 37071), diethoxyphosphotyrosine-modified peptides, YGGFL-OP and RARYEM-OP, for Biacore analysis produced at UNMC using chlorpyrifos oxon to label tyrosine,[7] SH-SY5Y human neuroblastoma cells (ATCC CRL-2266), N2a mouse neuroblastoma cells (ATCC CRL-131), bicinchoninic acid (BCA) Protein Assay Kit (Thermo Scientific #23225), poly(vinylidene fluoride) (PVDF) membrane 0.2 μm (Bio-Rad #162-0177), PD-10 desalting column 8.3 mL bed volume (Amersham Pharmacia Biotech #17-0851-01), precast 4−20% gradient polyacrylamide gels (Bio-Rad #4568094), YM-30 regenerated cellulose spin filter (Amicon #42410), and Durapore PVDF-0.45 μm centrifugal filter (Millipore UFC30HV00).

METHODS

Synthesis of Diethoxyphosphotyrosine (depY) Peptide Library

Peptides for immunization, B cell sorting, and screening of B cell clones were synthesized by van Grol and Fidder at TNO in The Netherlands. The structure of the depY peptide library for immunization and boosting is shown in Figure 1 (panel 1).

Conjugation of depY Peptide Library to Keyhole Limpet Hemocyanin Using Carbodiimide

For single B cell cloning, Syd Labs required ~5 mg keyhole limpet hemocyanin immunogen to be in phosphate-buffered saline (PBS) and to contain no precipitate and dimethyl sulfoxide. The keyhole limpet hemocyanin immunogen was prepared as follows. Fifty milligrams of keyhole limpet hemocyanin was weighed into a glass vial. Five milliliters of conjugation buffer (0.1 M 2-(*N*-morpholino)ethanesulfonic acid, 0.9 M NaCl, 0.02% sodium azide pH 4.7) was added. A portion of the keyhole limpet hemocyanin was dissolved. Undissolved solids settled to the bottom of the vial; 4.4 mL of the cloudy supernatant was transferred to a new glass vial, and 0.37 mL of 1-ethyl-3-[3-dimethylaminopropyl]carbodiimide hydrochloride (10 mg in 1 mL of water) and 10 mg of depY peptide library in 0.2 mL of dimethyl sulfoxide were added. The mixture was incubated overnight at room temperature. The conjugated keyhole limpet hemocyanin was dialyzed against 4 L of phosphate-buffered saline at 4 °C. The dialyzed conjugate was clarified by centrifugation, and 5.6 mL of a 2 mg/mL conjugated keyhole limpet hemocyanin (22%) was recovered.

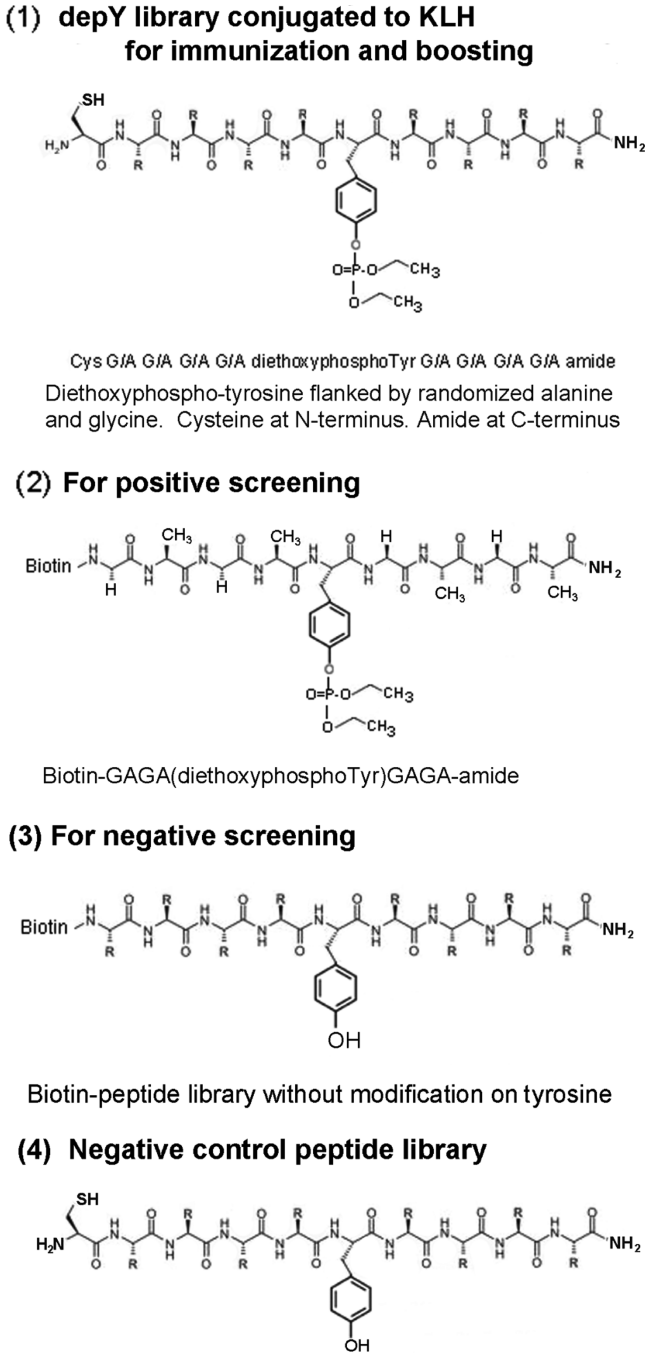

Figure 1. Structures of peptides for antibody production and screening. Tyrosine in panels (3) and (4) and the diethoxyphosphotyrosine in panel (1) were flanked by randomized alanine and glycine. Diethoxyphosphotyrosine in panel (2) was flanked by an exact sequence of alternating glycine and alanine residues.

Single B Cell Cloning Produces Rabbit Monoclonal 1C6

Syd Labs made monoclonal 1C6 by single B cell cloning using a proprietary protocol. The depY library conjugated to keyhole

https://doi.org/10.1021/acs.jproteome.1c00383
J. Proteome Res. 2021, 20, 4728−4745

limpet hemocyanin was used for immunization and boosting. The antigen concentration was 2 mg/mL in 2.8 mL. Syd Labs immunized two rabbits followed by four booster injections over a period of 3 months. Fresh splenocytes were isolated from the spleen of one rabbit. Splenocytes were sorted by flow cytometry to enrich antigen-recognizing B cells. A total of 1920 fluorescence-activated cell sorting (FACS)-sorted B cells were cultured in 96-well plates containing 1 cell/well for 14 days. Positive clones were identified by enzyme-linked immunosorbent assay (ELISA) in 96-well plates coated with biotin-GAGA(diethoxyphosphotyrosine)GAGA-NH_2 (Figure 1, panel 2). Out of 531 positive clones, 126 were picked for counterscreening with the biotinylated random peptide library without the modification on tyrosine (Figure 1, panel 3). Forty-five clones were positive with the biotinylated diethoxyphosphotyrosine peptide (structure in Figure 1, panel 2) and negative with the biotinylated peptide library without the modification on tyrosine (Figure 1, panel 3).

To ensure that positive rabbit single B cells secreted IgG, the supernatants of single B cell cultures were hybridized with anti-IgG secondary antibodies in ELISA. Only clones that bound the anti-IgG secondary antibody were selected for further confirmation and antibody sequencing.

Ten positive IgG clones were selected for antibody sequencing. The cDNA of six clones was ligated into expression plasmids. Transient expression yielded six purified antibodies, 100 μg each, for characterization by Biacore. The most reactive rabbit monoclonal, 1C6, was selected for expansion.

Binding Constants Evaluated by Biacore Analysis

Binding experiments were performed by U. Yerramalla at Precision Antibody (Columbia, MD) on a Biacore T-200 instrument at 25 °C. Each monoclonal was immobilized on a CM5 sensor chip using 1-ethyl-3-[3-dimethylaminopropyl]-carbodiimide hydrochloride/*N*-hydroxysuccinimide (EDC/NHS) in 10 mM sodium acetate pH 5. Unoccupied sites were blocked with 1 M ethanolamine. The immobilized antibodies were tested for binding to the following peptides, where OP is diethoxyphosphate covalently linked to the side chain of tyrosine: YGGFL-OP, YGGFL, RARYEM-OP, RARYEM, NH_2-C G/A G/A G/A G/A (dep-tyrosine) G/A G/A G/A G/A-NH_2 (structure in Figure 1, panel 1), and NH_2-C G/A G/A G/A G/A (tyrosine) G/A G/A G/A G/A-NH_2 (structure in Figure 1, panel 4). Peptides in 10 mM 2-[4-(2-hydroxyethyl)piperazin-1-yl]ethanesulfonic acid pH 7.4, 150 mM NaCl, 3 mM ethylenediaminetetraacetic acid (EDTA), and 0.05% (v/v) polyoxyethylenesorbitan were injected onto the chip at a flow rate of 30 μL/min. Peptide concentrations ranged from 12.4 to 1000 nM. After each assay, the chip was regenerated with 10 mM glycine pH 1.75. The surface plasmon resonance signal was recorded as a sensorgram and plotted in response units versus time. BIAevaluation T-200 software (v.2.0) was used to calculate the equilibrium binding affinity constant K_d. The accuracy of the analysis was determined by calculating χ^2 values based on a comparison of the actual sensorgram to the sensorgram generated by BIAnalysis software. A χ^2 value below 1 is highly significant.

Antibody Sequencing

Total RNA from cultured rabbit B cells was purified and used for cDNA synthesis. DNA fragments including the variable regions of the antibody heavy and light chains, leader sequences, and partial constant regions were amplified using 5′ RACE and nested polymerase chain reaction (PCR) and then subcloned into a plasmid vector. For each B cell sample, the DNA fragments in 10 plasmid DNAs, 5 for the heavy chain and 5 for the light chain, were sequenced. Complementarity-determining region (CDR) analysis was performed using the sequencing data and the IMGT/V-QUEST tool.

Protein Concentration

Protein concentration was determined with the BCA assay using bovine albumin as a standard.

Culturing SH-SY5Y Cells for Western Blots

Human neuroblastoma SH-SY5Y cells were grown in DMEM/F12 Glutamax, penicillin−streptomycin (pen−strep) containing 15% fetal bovine serum (FBS). When cells were 70−80% confluent, the medium was changed to DMEM/F12 Glutamax, pen−strep (no serum) with 10 μM retinoic acid in the absence or presence of 10 μM chlorpyrifos oxon. Cells were harvested from T75 flasks on day 4. The washed cell pellet from each T75 flask contained approximately 300 μg of protein.

Western Blot

Cell lysates were denatured with 2% sodium dodecyl sulfate (SDS), 50 mM dithiothreitol, 10% glycerol, and 0.002% bromophenol blue in a boiling water bath for 3 min. Precast 4−20% of polyacrylamide gradient gels were loaded with 10 μg of cell lysate protein per lane. Positive controls were 0.1 μg of human albumin (P02768) modified on tyrosine by chlorpyrifos oxon (Y162 21%, Y174 2%, Y425 5%, Y435 98%) and 0.1 μg of porcine tubulin (P02550) modified on tyrosine by chlorpyrifos oxon (Y83 9%, Y103 69%, Y108 42%, Y161 43%, Y172 14%, Y224 19%, Y262 16%, Y272 37%, Y282 10%, Y312 45%, Y357 7%, Y399 16%, Y408 18%). The location and percent modification of tyrosines in CPO-albumin and CPO-tubulin had been established by mass spectrometry (see the Supporting Information for Onder et al.).[7]

Proteins were separated by electrophoresis at 200 V for 40 min. Electrophoresed proteins were transferred to a PVDF membrane at 100 V for 1 h. The membrane was blocked in 5% nonfat dry milk dissolved in 20 mM Tris−Cl, 0.15 M NaCl pH 7.5 (Tris-buffered saline (TBS)) and incubated with mouse anti-depY monoclonal 3B9 (2.5 μg in 10 mL) for 16 h at 4 °C. The anti-depY monoclonal 3B9 is secreted by mouse hybridoma cells.[7] The same blot was reprobed with rabbit anti-depY monoclonal 1C6 (1 μg in 10 mL) in 5% nonfat dry milk in TBS, overnight at 4 °C. Blots were washed with TBST (20 mM Tris−Cl, 0.15 M NaCl, 0.05% Tween-20 (v/v) pH 7.5) and incubated with antimouse IgG-HRP or antirabbit IgG-HRP for 1 h. Blots were washed with TBST and developed with the Clarity Max Western ECL Substrate or Super Signal West Dura ECL reagents. Chemiluminescent images were acquired on the Azure c600 Biosystem.

Chlorpyrifos Oxon Instability in Cell Cultures

We wanted to know the stability of CPO in cell cultures. Live SH-SY5Y cells were exposed to chlorpyrifos oxon for 0−6 days at 37 °C in serum-free medium. The assay for CPO concentration was based on the principle that CPO is a stoichiometric inhibitor of butyrylcholinesterase activity.[9] The purified human butyrylcholinesterase with an activity of 10 units/mL (corresponding to 100×10^{-12} mol active sites) in a volume of 0.425 mL was used for the assay. For reference, butyrylcholinesterase was incubated with 10 μL aliquots of 10 μM CPO (100×10^{-12} mol CPO) for 1 h or more at room temperature. For comparison, 10 μL aliquots were taken from

https://doi.org/10.1021/acs.jproteome.1c00383
J. Proteome Res. 2021, 20, 4728−4745

SH-SY5Y in serum-free culture medium over a period of 6 days, where the CPO concentration at time zero was 10 μM. Butyrylcholinesterase activity was measured in 0.1 M potassium phosphate pH 7.0 containing 0.5 mM dithiobisnitrobenzoic acid and 1 mM butyrylthiocholine iodide at 25 °C by recording the increase in absorbance at 412 nm in 4 mL quartz cuvettes in a Gilford spectrophotometer interfaced to a Macintosh computer via a MacLab A/D converter (ADInstrument Inc.). A freshly prepared 10 μM CPO solution in buffer inhibited butyrylcholinesterase 99.9−100%. Inhibition potency diminished with time in cell culture, reflecting hydrolysis of CPO to inactive products.

Immobilization of Rabbit Monoclonal 1C6 on Sepharose Beads

Rabbit monoclonal 1C6 (6.6 mg) was linked to CNBr-activated Sepharose 4B (1.3 g powder) as follows. Preservatives were washed out of 1.3 g of CNBr-Sepharose powder with 25 mL of ice-cold 1 mM HCl. This washing also served to swell the gel. The swollen gel was washed with an ice-cold coupling buffer (0.15 M $NaHCO_3$, 0.5 M NaCl pH 8). All but 0.1 mL of liquid was removed from 4.6 mL of washed beads before addition of 2 mL of cold coupling buffer and 0.4 mL of 1C6 antibody (6.6 mg). The reaction tube was rotated at room temperature overnight. The quantity of the unbound antibody in the supernatant fluid was estimated from absorbance at 280 nm, where an antibody concentration of 1 mg/mL has an absorbance of 1.4. It was found that 96% of the antibody was bound. The beads were washed with high salt (1 M NaCl in 0.1 M potassium phosphate pH 7), low salt (20 mM Tris−Cl pH 7.5), buffer containing nonionic detergent (20 mM Tris−Cl, 0.15 M NaCl, 0.2% Tween-20), and phosphate-buffered saline containing 0.05% of sodium azide. The washed beads were stored at 4 °C in phosphate-buffered saline plus 0.05% of azide. A 0.2 mL suspension contained 42 μg of monoclonal 1C6 and a bead volume of 20 μL.

Sample Preparation of SH-SY5Y Cells for Immunopurification on 1C6 Beads Followed by Liquid Chromatography Tandem Mass Spectrometry (LC-MS/MS)

SH-SY5Y cells in T75 flasks containing DMEM/F12 Glutamax, pen−strep (no serum), were treated with 10 μM retinoic acid and 10 μM CPO and incubated for 2 days at 37 °C in a humidified chamber with 5% CO_2. Cells from 14 T75 flasks were combined into one 15 mL tube where they were lysed with 0.6 mL of IP lysis buffer (25 mM Tris−Cl pH 7.4, 150 mM NaCl, 1% NP-40, 1 mM EDTA, 5% glycerol) and Halt protease inhibitor cocktail. Proteins were reduced with 10 mM dithiothreitol, alkylated with 50 mM iodoacetamide and desalted by passage through a G25 Sepharose column equilibrated with 20 mM ammonium bicarbonate. The nonionic detergent NP-40 did not separate from proteins on the desalting column. Desalted samples were concentrated 3-fold, raising the NP-40 concentration to 3%. A 0.29 mL aliquot with a protein concentration of 0.67 mg/mL in 20 mM ammonium bicarbonate (194 μg) was digested with 4 μg trypsin at 37 °C for 16 h. Trypsin was inactivated in a boiling water bath for 3 min.

Tryptic peptides (194 μg in 0.29 mL of 20 mM NH_4HCO_3, 3% NP-40) were incubated with immobilized antibody 1C6 (105 μg monoclonal 1C6 on 50 μL Sepharose beads in 0.5 mL PBS, plus 0.01% azide) overnight at room temperature on a rotating mixer. The beads were washed four times with 1 mL PBS and three times with 1 mL water on 0.45 μm PVDF spin filters that retained the beads and the bound peptides on the PVDF membrane. Bound peptides were released by incubating the washed beads with 0.2 mL of 50% acetonitrile, plus 1% formic acid for 1.5 h. Peptides were recovered by centrifuging the 0.45 μm PVDF spin filter, leaving beads on the membrane while eluting peptides. The peptide volume was reduced to 24 μL in a vacuum centrifuge. Samples were centrifuged for 20 min at 14 000g before the top 12 μL were transferred to autosampler vials.

Sample Preparation of N2a Cells for Immunopurification on 1C6 Beads Followed by Liquid Chromatography Tandem Mass Spectrometry

Mouse N2a cells in 100 mm dishes were treated with 0, 10, or 100 μM chlorpyrifos oxon in serum-free Opti-MEM for 24 h. Cells were lysed with 500 μL IP lysis buffer containing Halt protease inhibitor. Lysates were centrifuged at 4 °C for 20 min at 13 000g. Protein concentrations in the supernatants were 4.3 mg/mL for control and 2.2 mg/mL for treated cells. Soluble proteins in the supernatants were reduced with 10 mM dithiothreitol in a boiling water bath; the heating step caused the mouse proteins to precipitate. The pellet was dissolved in 100 μL of 8 M urea. The dissolved pellet and supernatant were alkylated with 50 mM iodoacetamide and desalted by filtration through a YM-30 spin filter. Proteins captured on the filter were digested with 1 μg of trypsin (2.5 μL of 0.4 μg/μL trypsin) in 0.1 mL of 20 mM ammonium bicarbonate at 37 °C overnight. Tryptic peptides were collected into new tubes by centrifuging the digests through the YM-30 spin filter. The filter was washed twice with 100 μL of 20 mM ammonium bicarbonate to recover more peptides. The 300 μL tryptic peptide samples were incubated with a 0.5 mL suspension containing 105 μg of immobilized 1C6 monoclonal conjugated to 50 μL of Sepharose beads. After a 16 h rotation at room temperature, the beads were washed 3× with PBS and 3× with water on 0.45 μm spin filters. The 0.45 μm spin filters were used because washing on the filters recovered more beads. Peptides were released from antibody binding by incubating the washed beads on the filter with 0.2 mL of 50% acetonitrile, 1% formic acid for 1 h followed by centrifugation. The flowthrough was collected into a new tube. The extraction step was repeated with a second aliquot of 0.2 mL of 50% acetonitrile and 1% formic acid. Samples were dried by vacuum centrifugation, dissolved in 50 μL of 0.1% formic acid, and centrifuged to pellet particulates. The top 10 μL were transferred to autosampler vials.

LC-MS/MS Orbitrap Fusion Lumos Tribrid Mass Spectrometer (Thermo Fisher Scientific)

Peptides were separated by C18 chromatography and sprayed directly into the Orbitrap Fusion Lumos mass spectrometer. Chromatography was performed with a Thermo RSLC Ultimate 3000 ultrahigh pressure liquid chromatography system (Thermo Scientific) using 0.1% formic acid in water (solvent A) and 0.1% formic acid in 70% acetonitrile (solvent B) at 36 °C. A 5 μL aliquot of peptides was applied to an Acclaim PepMap 100 C18 trap column (75 μm × 2 cm; Thermo Scientific cat# 165535) at 4 μL/min and washed with 0.1% formic acid in 2% acetonitrile for 10 min. The flow was switched to a Thermo Easy-Spray PepMap RSLC C18 separation column (75 μm × 50 cm with 2 μm particles, Thermo Scientific cat# ES803), and the flow rate was reduced to 300 nL/min. Peptides were eluted with a linear gradient from 3 to 70% solvent B over 50 min followed by 70−99%

https://doi.org/10.1021/acs.jproteome.1c00383
J. Proteome Res. 2021, 20, 4728−4745

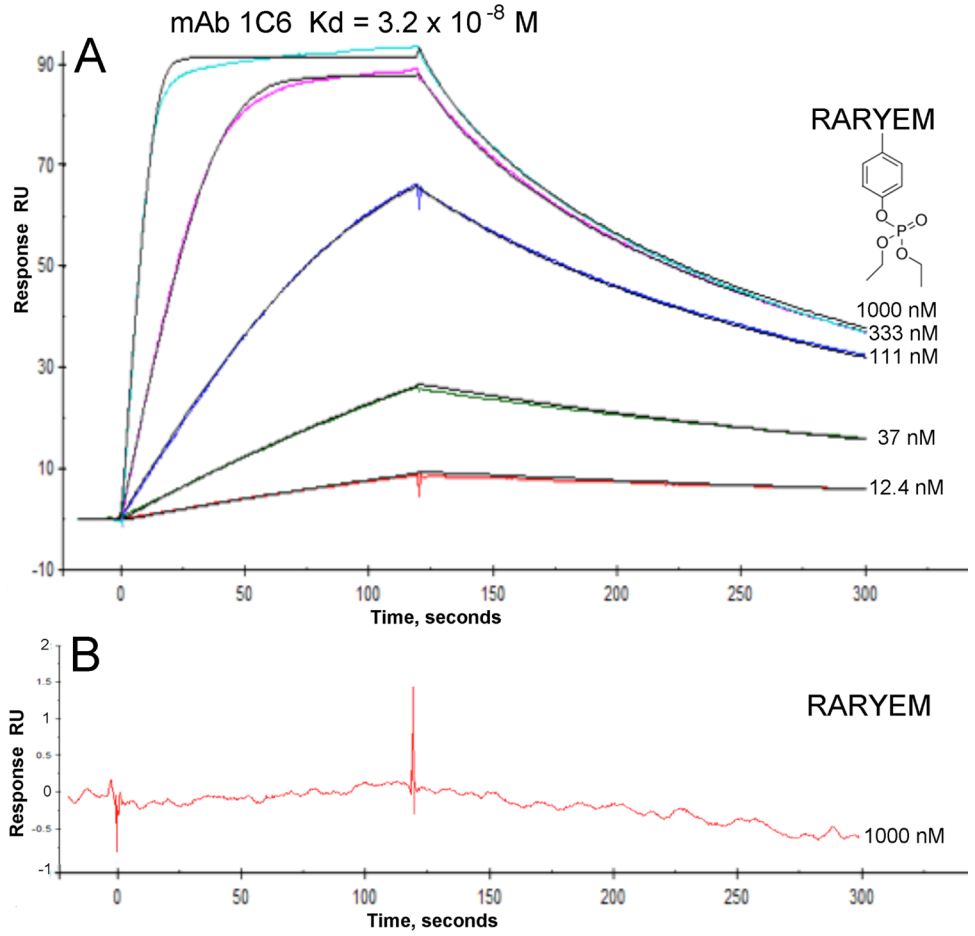

Figure 2. Biacore measurement of the binding affinity of monoclonal 1C6. (A) Binding of diethoxyphosphotyrosine peptide RARY$_{OP}$EM (where OP is diethoxyphospho). The association rate constant k_{on} is 4.12×10^5 M^{-1} s^{-1}. The dissociation rate constant k_{off} is 0.01307 s^{-1}. The equilibrium affinity constant $K_d = 3.2 \times 10^{-8}$ M was calculated by dividing k_{off}/k_{on}. The χ^2 value of 0.369 is highly significant. (B) Control peptide RARYEM did not bind to monoclonal 1C6. Wavy lines are observed data, and solid lines are fitted data.

solvent B over 4 min and a wash with 99% solvent B for 4 min. The level of solvent B was reduced from 99 to 3% over 4 min, and the column was re-equilibrated with 3% solvent B for 15 min.

Data were collected using data-dependent acquisition. A full survey scan from 350 to 1800 m/z was acquired in the Orbitrap with a resolution of 120 000. The automatic gain control for setting the ion population in the Orbitrap before collecting the MS was set at 4×10^5, and the ion filling time was set to 100 ms. The 25 most intense ions with a charge state of 2−6 were isolated in a 3 s cycle and fragmented using high-energy collision-induced dissociation with 35% normalized collision energy. Fragment ions were detected in the Orbitrap with a mass resolution of 30 000 at 200 m/z. The automatic gain control target for the MS/MS was set at 5×10^4, an ion filling time at 60 ms, and the dynamic exclusion was set to 30 s with a 10 ppm mass window. Data were reported in *.raw format.

Protein Prospector Search for Diethoxyphosphate Adducts on Tyrosine

The *.raw data files from the Orbitrap Fusion Lumos were converted to *.mgf files using MSConvert (ProteoWizard Tools from SourceForge). The *.mgf files were analyzed using Batch-Tag Web on the Protein Prospector website https://prospector.ucsf.edu.

The search parameters added to the Batch-Tag page in Protein Prospector were as follows: Database: SwissProt 2017.11.01 or SwissProt 2020.09.02 or NCBInr 2013.6.17. Taxonomy: *Homo sapiens* or *Mus musculus*. Digest: trypsin, constant mods: carbamidomethyl (C), variable mods: oxidation (M), user-defined variable modifications Mod 1 label: depY. Mod 1 Elem Comp: C4H9P1O3, specificity: Y. Mass modification range: 135−137, parent tolerance: 20 ppm, fragment tolerance: 30 ppm. Instrument: ESI-Q-high res. Expectation calc method: none. A checkmark in box uncleaved avoids reports of peptides cleaved at the modified lysine. The software provided a list of modified peptides, the retention time of each modified peptide, statistical scores reflecting confidence, mass and charge state of the parent ion, percent matched intensity, protein accession number, amino acid number of the modified residue, MS/MS spectra of the modified peptide, and a list of theoretical and observed fragment ions for each modified peptide. We manually evaluated each MS/MS spectrum to identify false positives.

Protein Prospector Search for Phosphorylated Tyrosine

The search parameters for phosphorylated tyrosine were the same as above with two exceptions. The box for elementary composition was changed to Elem Comp P1O3H1 and the mass modification range was changed to 79−81.

https://doi.org/10.1021/acs.jproteome.1c00383
J. Proteome Res. 2021, 20, 4728−4745

Table 1. Binding Constants to Diethoxyphosphotyrosine Peptides

monoclonal	target	k_{on} (M^{-1} s^{-1})	k_{off} (s^{-1})	K_d (M)	χ^2 [b]
rabbit 1C6	$RARY_{OP}EM$	4.12×10^5	0.01307	3.2×10^{-8}	0.369
rabbit 1C6	depY peptide library	3.69×10^7	0.000431	1.17×10^{-11}	0.478
rabbit 2C9	$RARY_{OP}EM$	5.23×10^5	0.009681	1.85×10^{-8}	1.6
mouse 3B9 depY[a]	$PPY_{OP}RM$			36×10^{-8}	0.361

[a]Mouse 3B9 depY monoclonal was described by Onder et al.[7] [b]χ^2 values below 1 are highly significant. The fit between the observed and theoretical kinetic curves was reported as the standard error. The standard error ranged from 0.5 to 2% of the response unit (RU). See Figure 2A for a comparison of observed and theoretical response units.

>1C6_Heavy chain MZ086765
METGLRWLLLVAVLKGVQCQSLEESGGDLVKPGASLTLTCTASGFSISSAYGMCWVRQAPGK
GLEWIASIYAGVGASAYYANWAKGRFTISRTSSTTVTLQMTSLTAADTATYFCARGYIGDGYAA
GAFDPWGPGTLVTVSS\GQPKAPSVFPLAPCCGDTPSSTVTLGCLPEPVTVTWNSGTLTNGVR
TFPSVRQSSGLYSLSSVVSVTSSSQPVTCNVAHPATNTKVDKTVAPSTCSKPMCPPPELPGGP
SVFIFPPVKGYLKPKDTLMISRTPEVTCVVVDVSQDDPEVQFTWYINNEQVRTARPPLREQQFN
STIRVVSTLPIAHQDWLRGKEFKCKVHNKALPAPIEKTISKARGQPLEPKVYTMGPPREELSSRS
VSLTCMINGFYPSDISVEWEKNGKAEDNYKTTPTVLDSDGSYFLYSKLSVPTSEWQRGDVFTC
SVMHEALHNHYTQKSISRSPGK

>2C9_Heavy chain MZ086767
METGLRWLLLVAVLKGVQCQEQLVESGGGLVQPGASLTLTCKASGFSISSVYGMCWVRQAPG
KGLEWIASIYAGVGASTYYANWAKGRFTISRTSSTTVTLQMTSLTAADTATYFCARGFIGDGYAA
GAFDPWGPGTLVTVSS\GQPKAPSVFPLAPCCGDTPSSTVTPGCLVKGYLPEPVTVTWNSGTL
TNGVRTFPSVRQSSGLYSLSSVVSVTSSSQPVTCNVAHPATNTKVDKTVAPSTCSKPMCPPPE
LPGGPSVFIFPPKPKDTLMISRTPEVTCVVVDVSQDDPEVQFTWYINNEQVRTARPPLREQQFN
STIRVVSTLPIAHQDWLRGKEFKCKVHNKALPAPIEKTISKARGQPLEPKVYTMGPPREELSSRS
VSLTCMINGFYPSDISVEWEKNGKAEDNYKTTPTVLDSDGSYFLYSKLSVPTSEWQRGDVFTC
SVMHEALHNHYTQKSISRSPGK

>1C6_Light chain MZ086766
MDTRAPTQLLGLLLLWLPGARCALVMTQTPASVEVAVGGTVTIKCQASENIYYSLAWYQQKPG
QRPKLLIYKASTLASGVPSRFKGSRSGTEFTLTISDLECADAATYYCQQGYTGTNVESAFGGGT
EVVVK\GDPVAPTVLIFPPAADQVATGTVTIVCVANKYFPDVTVTWEVDGTTQTTGIENSKTPQN
SADCTYNLSSTLTLTSTQYNSHKEYTCKVTQGTTSVVQSFNRGDC

>2C9_Light chain MZ086768
MDTRAPTQLLGLLLLWLPGARCALVMTQTPASVEVAVGGTVTIKCQANENIYYSLAWYQQKPG
QRPKLLIYKASTLASGVPSRFKGSRSGTEFTLTISDLECADAATYYCQQGYTGTNVESAFGGGT
EVVVA\GDPVAPTVLIFPPAADQVATGTVTIVCVANKYFPDVTVTWEVDGTTQTTGIENSKTPQN
SADCTYNLSSTLTLTSTQYNSHKEYTCKVTQGTTSVVQSFNRGDC

Figure 3. Amino acid sequences of rabbit monoclonals 1C6 and 2C9. Complementarity-determining regions are shown in red. A slash mark indicates the start of the constant regions. GenBank accession numbers are MZ086765 for 1C6 heavy chain, MA086766 for 1C6 light chain, MZ086767 for 2C9 heavy chain, and MZ086768 for 2C9 light chain.

Protein Prospector Search for Dichlorvos Adducts on Tyrosine

Dichlorvos adducts carry a dimethoxyphosphate group. The search parameters for dichlorvos adducts on tyrosine were modified to Elem Comp P1C2H5O3, mass modification range 107−109.

Proteome Discoverer Search for Diethoxyphosphate Adducts on Tyrosine, Serine, Threonine, and Lysine

Database searching was performed with Proteome Discoverer v 2.4 (Thermo Scientific). The processing method was PWF_Tribrid_Basic_Sequest HT. Parameters for the Spectrum Files RC node were protein database either *H. sapiens* SwissProt 20200706 or *M. musculus* UniProt 11-24-2020; the enzyme was trypsin full; static modification was carbamidomethyl Cys; and all others were default. Parameters for the Spectrum Selector node were default. Parameters for the Sequest HT node were protein database either *H. sapiens* SwissProt 20200706 or *M. musculus* UniProt 11-24-2020; the enzyme was trypsin full; the precursor mass tolerance was 10 ppm; the fragment mass tolerance was 0.02 Da; dynamic modifications were oxidized Met, diethylphosphate Ser, Thr, Tyr, Lys, ethylphosphate Ser, Thr, Tyr, Lys, *O*-dimethylphosphate Ser, Thr, Tyr, Lys, and *O*-methylphosphate Ser, Thr, Tyr, Lys; static modification was carbamidomethyl Cys; and all others were default. The fixed value PSM validator was replaced with target decoy PSM validator, and default parameters were used.

The consensus method was CWF_Basic with nodes MSF Files, PSM Grouper, Peptide Validator, Peptide and Protein Filter, Protein Scorer, and Protein Grouping. Default parameters were used for all nodes. The significance threshold of the ion score was calculated based on a false discovery rate of ≤1%.

https://doi.org/10.1021/acs.jproteome.1c00383
J. Proteome Res. 2021, 20, 4728−4745

Criteria to Manually Assess and Exclude False Positives from the MS/MS Results

The criteria for accepting a potential diethoxyphosphotyrosine peptide were as follows. Fragment ions in the MS/MS spectrum contained an added mass of 136.03 Da. The % matched intensity was greater than 45%. The XCorr value was in the range of 1−6. A minimum of two fragment ions were in a series (for example, y4, y5) and were at least 2-fold above background. The charge state of fragment ions was lower than that of the parent ion.

The criteria for excluding a potential depY peptide were as follows. MS/MS spectra had no fragment ions with an added mass of 136.03 Da. The % matched intensity was less than 45%. The XCorr value was less than 1. Candidate fragment ions in the same charge state as the parent ion were rejected. Parent ions in charge state +6 were excluded.

The mass spectrometry data have been deposited to the ProteomeXchange Consortium via the PRIDE[10] partner repository with the data set identifier PXD027203.

RESULTS

The structures of peptides for antibody production, screening, and evaluation are shown in Figure 1. The peptide libraries containing randomized glycine and alanine residues were designed to minimize an antibody response to the peptide backbone, a strategy successfully used by Fuhs et al.[11] to produce monoclonals specific for phosphohistidine. Chemists synthesized 100 mg of the structures in Figure 1 panels 1, 3, and 4 and 2.7 mg of the biotinylated peptide in panel 2. The depY library in panel 1, after being conjugated to keyhole limpet hemocyanin, was used for immunization and boosting. The biotinylated peptide in panel 2 was used in ELISA to identify positive single B cell clones. The biotinylated peptide in panel 3 was used in ELISA to identify clones that were not selective for the diethoxyphosphate adduct on tyrosine. The peptide library in panel 4 was used as a negative control in Biacore assays where the positive analyte was the depY library in panel 1.

Single B Cell Monoclonal Antibodies

The Methods section summarizes the steps from immunizing two rabbits through isolation of single B cells from the splenocytes of one rabbit by FACS, identification of positive clones by ELISA, antibody sequencing of 10 clones, expression and purification of antibodies from 6 clones, and evaluation of 6 monoclonals by measurement of binding constants on the Biacore instrument.

Biacore Values for Binding Constants

Scouting assays with 1000 nM Y_{OP}GGFL (where OP is diethoxyphospho) tested six monoclonals for relative binding to the diethoxyphosphotyrosine peptide compared to that of the unmodified peptide, YGGFL. Two promising clones were identified: 1C6 and 2C9. Monoclonals 1C6 and 2C9 were further evaluated by measuring binding to peptides RAR-Y_{OP}EM and RARYEM. This second set of peptides was used after the initial set had been consumed. On and off rates were measured for peptide concentrations ranging from 12.4 to 1000 nM. The sensorgram for monoclonal 1C6 in Figure 2A shows that the diethoxyphosphorylated peptide binds tightly with a K_d value of 3.2×10^{-8} M. In contrast, the unmodified peptide RARYEM in Figure 2B does not bind to monoclonal 1C6.

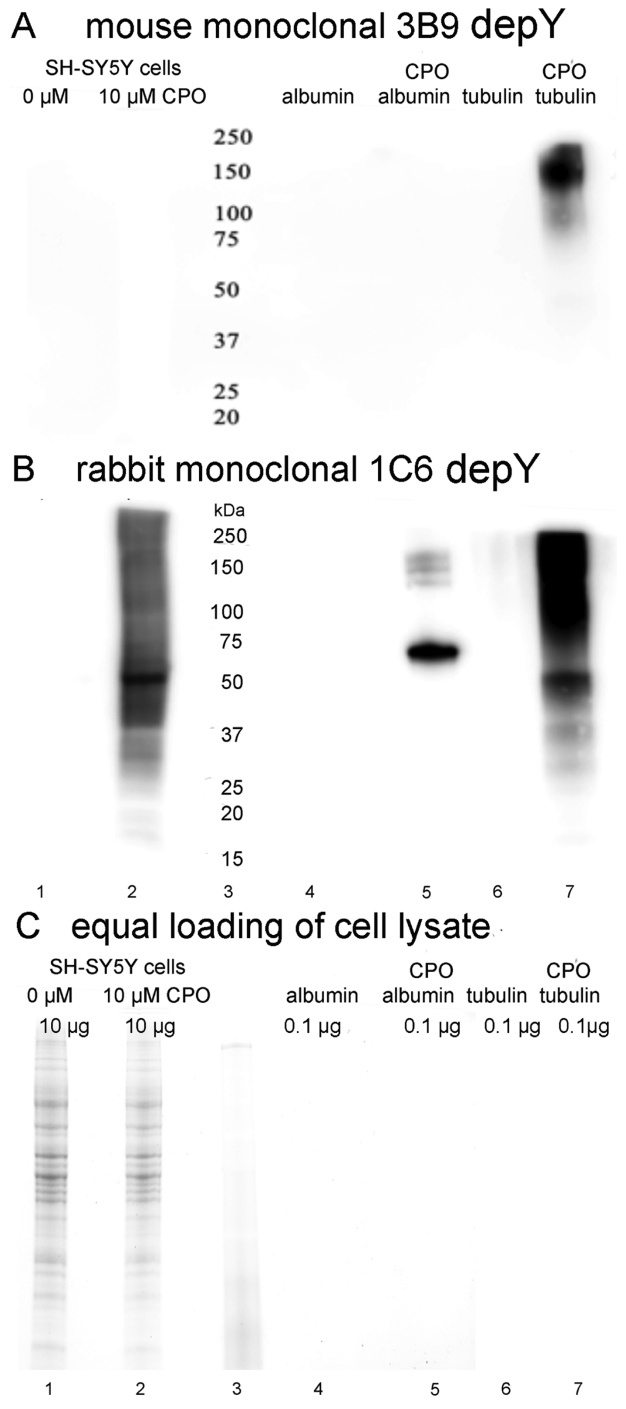

Figure 4. Western blot of SH-SY5Y cell lysates hybridized with antidiethoxyphosphotyrosine monoclonals 3B9 and 1C6. Cells incubated in serum-free medium containing 10 μM retinoic acid without or with 10 μM chlorpyrifos oxon (CPO) were harvested on day 2. (A) Blot was probed with mouse monoclonal 3B9. (B) The same blot was reprobed with rabbit monoclonal 1C6. Images were acquired on an Azure c600 gel imaging system with ECL Super Signal West Dura (Thermo Scientific 37071). (C) Azure c600 image of proteins detected in the Bio-Rad stain-free gel in which proteins are made fluorescent by reaction with a gel-embedded ligand. Cell lysates were loaded at 10 μg protein per lane, in lanes 1 and 2. Positive controls CPO-albumin and CPO-tubulin and negative controls albumin and tubulin, in lanes 4−7, were loaded at 0.1 μg per lane, quantities too low for detection in the stain-free gel.

https://doi.org/10.1021/acs.jproteome.1c00383
J. Proteome Res. 2021, 20, 4728−4745

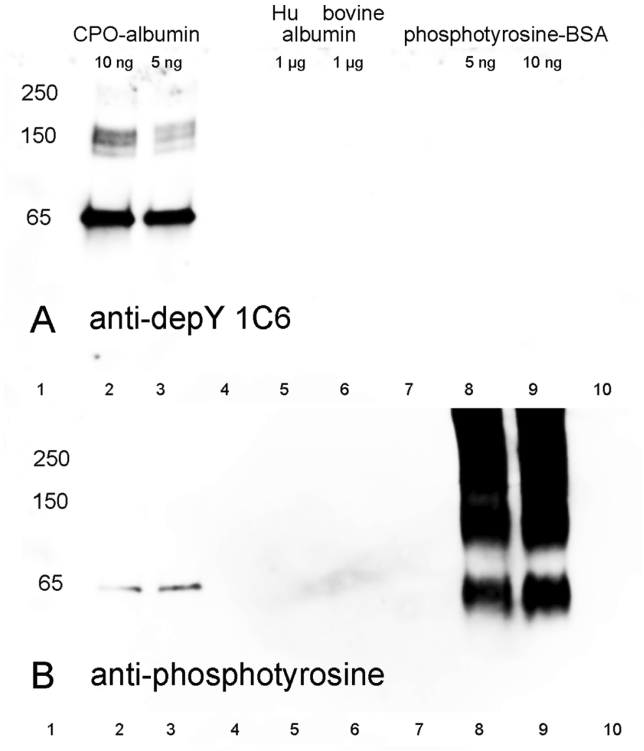

Figure 5. Western blot shows binding of anti-depY IC6 to diethoxyphosphotyrosine-albumin (CPO-albumin) but not to phosphotyrosine albumin. (A) Anti-depY 1C6 recognizes CPO-albumin in lanes 2 and 3 but not control human and bovine albumin in lanes 5 and 6 and not phosphotyrosine-BSA in lanes 8 and 9. (B) The same blot was reprobed with antiphosphotyrosine antibody without stripping the blot. Phosphotyrosine adducts on albumin are recognized in lanes 8 and 9. Weak bands at 65 kDa in lanes 2 and 3 are residual bands from panel (A).

Similar results were obtained for monoclonal 2C9: association rate constant, k_{on} = 5.23 × 10^5 M^{-1} s^{-1}; and dissociation rate constants, k_{off} = 0.009681 s^{-1} and K_d = 1.85 × 10^{-8} M. A χ^2 value of 1.6 for 2C9 was higher than a χ^2 value of 0.369 for 1C6. Monoclonal 1C6 was selected for large-scale expression and purification.

Binding constants for monoclonal 1C6 were also measured for the depY peptide library (structure 1 in Figure 1) and the negative control peptide library (structure 4 in Figure 1). The analyte concentrations ranged from 0.313 to 5 nM. The values for the depY peptide library were k_{on} = 3.69 × 10^7 M^{-1} s^{-1}, k_{off} = 4.31 × 10^{-4} s^{-1}, K_d = 1.17 × 10^{-11} M, and χ^2 = 0.478. The negative control peptide library did not bind to monoclonal 1C6. Binding constants are summarized in Table 1.

Amino Acid Sequences

The complete amino acid sequences of the variable and constant regions of the heavy and light chains of rabbit monoclonals 1C6 and 2C9 are shown in Figure 3. The complementarity-determining regions (CDRs) of the heavy chains of rabbit monoclonals 1C6 and 2C9 (shown in red) are similar but not identical. They differ by one amino acid, Y158 in 1C6 versus F158 in 2C9. The light chain CDRs are identical in both monoclonals shown in red (see Figure 3).

Western Blots

Monoclonal antibodies specific for diethoxyphospho adducts on tyrosine were used to determine whether proteins inside a live cell become modified by chlorpyrifos oxon added to serum-free culture medium. In Figure 4A, mouse monoclonal 3B9 failed to detect adducts in SH-SY5Y cells treated with 10 µM CPO (lane 2) but did detect the CPO-tubulin positive control in lane 7. The same blot was reprobed with rabbit monoclonal 1C6 in Figure 4B. The SH-SY5Y cell lysate in lane 2 gave signals for proteins ranging in molecular weight from 25 to 300 kDa. The most intense signal was for 50 kDa proteins. Monoclonal 1C6 also recognized 0.1 µg of the positive control CPO-albumin in lane 5 and had a strong response to the 0.1 µg of positive control CPO-tubulin in lane 7. Monoclonal 1C6 did not recognize proteins in untreated cell lysate (lane 1), untreated albumin (lane 4), and untreated tubulin (lane 6). It was concluded that CPO could enter living SH-SY5Y cells and that many proteins in cultured cells are modified when chlorpyrifos oxon is added to the culture medium at a dose of 10 µM. The comparison between monoclonals 3B9 and 1C6 shows that monoclonal 1C6 is more sensitive and likely more useful for identifying proteins modified by chlorpyrifos oxon.

In Figure 4B (lane 7), CPO-treated tubulin has been transformed from its original 50 kDa mass to high-molecular-weight aggregates. In previous reports,[12,13] we showed that CPO catalyzes the formation of covalent isopeptide cross-links between diethoxyphospholysine and glutamic acid or diethoxyphospholysine and aspartic acid, with the release of diethoxyphosphate. The cross-linking reaction results in high-molecular-weight protein aggregates. Not all diethoxyphospholysine adducts participate in a cross-linking reaction; those that retain the adduct are detectable by mass spectrometry.[13] To date, we have not observed a cross-linking reaction involving diethoxyphosphotyrosine adducts.

CPO-treated albumin in Figure 4B (lane 5) also has high-molecular-weight aggregates, but they are low in abundance. Albumin is less susceptible to chlorpyrifos oxon-catalyzed cross-linking than tubulin.

The Western blot in Figure 5A shows that anti-depY 1C6 specifically recognizes the diethoxyphosphate adduct on tyrosine (CPO-albumin in lanes 1 and 2) but does not recognize phosphorylated tyrosine (lanes 8 and 9). The phosphotyrosine adduct on bovine albumin is recognized in Figure 5B by antiphosphotyrosine antibody. The broad positive band for phosphotyrosine-bovine serum albumin (BSA) in Figure 5B reflects the fact that we synthesized the adduct with the aid of carbodiimide. The procedure for synthesis of phosphotyrosine-BSA is described in the Supporting Information section. Carbodiimide cross-linked phosphotyrosine to albumin and also cross-linked albumin molecules to each other to form high-molecular-weight forms of phosphotyrosine albumin adducts.

The Western blot in Figure S1 in the Supporting Information section shows that anti-depY 1C6 specifically recognizes proteins modified by CPO but does not recognize proteins modified by dichlorvos. The proteins in Figure S1 were from SH-SY5Y cells treated with either 10 µM CPO or 10 µM dichlorvos.

The Western blot results were supported by Protein Prospector searches of mass spectrometry data. Immunopurified peptides from CPO-treated SH-SY5Y cells contained abundant diethoxyphospho adducts on tyrosine (from CPO), but no dimethoxyphospho adducts (from dichlorvos), and only one phosphorylated tyrosine.

https://doi.org/10.1021/acs.jproteome.1c00383
J. Proteome Res. 2021, 20, 4728−4745

Table 2. Diethoxyphosphate Adducts on Tyrosine in Human SH-SY5Y Neuroblastoma Cells Treated with 10 μM Chlorpyrifos Oxon for 2 days

no.	peptide	modification	accession[a]	protein	MH^+ (Da)[b]	m/z (Da)[c]	% matched intensity[d]
1	YPIEHGIITNWDDMEK	oxidation [M14]; diethoxyphosphate [Y1]	P68032	actin, α cardiac muscle 1	2112.9348	704.9828	44.8
2	DSYVGDEAQSK	diethoxyphosphate [Y3]	P60709	actin, cytoplasmic 1	1334.5512	667.7790	52.3
3	GYSFTTTAER	diethoxyphosphate [Y2]	P60709	actin, cytoplasmic 1	1268.5559	634.7817	83.5
4	KYSVWIGGSILASLSTFQQMWISKPEYDEAGPSIVHR	diethoxyphosphate [Y27]	P63267	actin, γ-enteric smooth muscle	4229.1199	846.6298	72.2
5	IIAPPERKYSVWIGGSILASLSTFQQMWISKPEYDEAGPSIVHR	oxidation [M27]; diethoxyphosphate [Y34]	P63267	actin, γ-enteric smooth muscle	5021.5714	1005.1201	69.6
6	AQVVYYSEMHK	diethoxyphosphate [Y5]	Q9NQY0	bridging integrator 3	1490.6749	497.5631	64.2
7	AQVVYYSEMHK	diethoxyphosphate [Y6]	Q9NQY0	bridging integrator 3	1490.6749	497.5631	66.9
8	MIYASSK	diethoxyphosphate [Y3]	P23528	cofilin-1	935.4307	468.2190	55.9
9	YALYDATYETK	diethoxyphosphate [Y1]	P23528	cofilin-1	1473.6549	737.3313	47.8
10	YALYDATYETK	diethoxyphosphate [Y4]	P23528	cofilin-1	1473.6549	737.3313	57.6
11	LPLQDVYK	diethoxyphosphate [Y7]	P68104	elongation factor 1-α 1	1111.5799	556.2938	72.7
12	LIINSLYK	diethoxyphosphate [Y7]	P14625	endoplasmin	1099.6163	550.3118	65.9
13	IYVLLR	diethoxyphosphate [Y2]	P84090	enhancer of rudimentary homologue	912.5318	456.7693	56.8
14	VLLPEYGGTK	diethoxyphosphate [Y6]	P61604	10 kDa heat shock protein, mitochondrial	1212.6276	606.817	82.4
15	LLVVYPWTQR	diethoxyphosphate [Y5]	P02042	hemoglobin	1410.7545	705.8810	88.7
16	AAEVYTR	diethoxyphosphate [Y5]	Q7Z4V5	hepatoma-derived growth factor-related protein 2	945.4441	473.2256	83.2
17	NYYEQWGK	diethoxyphosphate [Y2]	P22626	heterogeneous nuclear ribonucleoproteins A2/B1	1223.5133	612.2602	68.4
18	QVMYQQSSGR	oxidation [M3]; diethoxyphosphate [Y4]	Q9UM22	mammalian ependymin-related protein 1	1335.5763	668.2920	54.3
19	ILYSQCGDVMR	carbamidomethyl [C6]; oxidation [M10]; diethoxyphosphate [Y3]	P60660	myosin light polypeptide 6	1493.6528	747.3301	76.3
20	LEPQIASASEYAHR	diethoxyphosphate [Y11]	O60664	perilipin-3	1707.8102	569.9420	57.1
21	LVGYLDR	diethoxyphosphate [Y4]	P07602	prosaposin	971.4961	486.2518	77.0
22	YYTPTISR	diethoxyphosphate [Y1]	P49721	proteasome subunit β type-2	1136.5388	568.7729	58.1
23	YYTPTISR	diethoxyphosphate [Y2]	P49721	proteasome subunit β type-2	1136.5388	568.7729	55.6
24	YKPESEELTAER	diethoxyphosphate [Y1]	P07237	protein disulfide isomerase	1587.7310	529.9152	60.7
25	SYYLKPSK	diethoxyphosphate [Y2]	Q9UFN0	protein NipSnap homologue 3A	1121.5642	374.5261	63.1
26	SYYLKPSK	diethoxyphosphate [Y3]	Q9UFN0	protein NipSnap homologue 3A	1121.5642	374.5261	52.6
27	KLPEEEAECYFHSR	carbamidomethyl [C9]; diethoxyphosphate [Y10]	Q9NVS9	pyridoxine-5′ phosphate oxidase	1930.8413	644.2853	57.0
28	AYLESEVAISEELVQK	diethoxyphosphate [Y2]	Q9NQC3	reticulon-4	1943.9613	648.6584	94.7
29	YSNSALGHVNCTIK	carbamidomethyl [C11]; diethoxyphosphate [Y1]	Q9NQC3	reticulon-4	1699.7873	567.2673	47.5
30	PLISVYSEK	diethoxyphosphate [Y6]	P36578	60S ribosomal protein L4	1171.6021	586.3047	64.2
31	AFGYYGPLR	diethoxyphosphate [Y4]	P84103	serine/arginine-rich splicing factor 3	1179.5598	590.2835	82.0
32	AFGYYGPLR	diethoxyphosphate [Y5]	P84103	serine/arginine-rich splicing factor 3	1179.5598	590.2835	84.0
33	NLDIERPTYTNLNR	diethoxyphosphate [Y9]	Q71U36	tubulin α-1A chain	1854.911	618.9753	87.4
34	TGTYR	diethoxyphosphate [Y4]	Q71U36	tubulin α-1A chain	733.3281	367.1677	56.8
35	EDAANNYAR	diethoxyphosphate [Y7]	Q71U36	tubulin α-1A chain	1159.4779	580.2423	56.4
36	ISVYYNEATGGK	diethoxyphosphate [Y4]	P07437	tubulin β chain	1437.6661	719.3364	91.3
37	ISVYYNEATGGK	diethoxyphosphate [Y5]	P07437	tubulin β chain	1437.6661	719.3364	77.0

https://doi.org/10.1021/acs.jproteome.1c00383
J. Proteome Res. 2021, 20, 4728−4745

Table 2. continued

no.	peptide	modification	accession[a]	protein	MH$^+$ (Da)[b]	m/z (Da)[c]	% matched intensity[d]
38	GHYTEGAELVDSVLDVVR	diethoxyphosphate [Y3]	P07437	tubulin β chain 4B	2095.0107	699.0085	98.2
39	GSQQYR	diethoxyphosphate [Y5]	P07437	tubulin β chain 4B	874.3817	437.6945	48.5
40	INVYYNEATGNK	diethoxyphosphate [Y4]	Q9BVA1	tubulin β-2B chain	1521.6985	761.3534	62.3
41	INVYYNEATGNK	diethoxyphosphate [Y5]	Q9BVA1	tubulin β-2B chain	1521.6985	761.3534	59.5
42	IREEYPDR	diethoxyphosphate [Y5]	Q9BVA1	tubulin β-2B chain	1213.5613	405.1918	58.2
43	INVYYNEATGGK	diethoxyphosphate [Y4]	P68371	tubulin β-4B chain	1464.6771	732.8420	62.3
44	INVYYNEATGGK	diethoxyphosphate [Y5]	P68371	tubulin β-4B chain	1464.6771	732.8420	59.5
45	VTQSDLYK	diethoxyphosphate [Y7]	O43399	tumor protein D54	1089.5228	545.2648	52.7
46	YFNSVTLTGR	diethoxyphosphate [Y1]	Q96IX5	upregulated during skeletal muscle growth protein 5	1357.6181	679.3127	54.5
47	SVSSSSYR	diethoxyphosphate [Y7]	P08670	vimentin	1008.4398	504.7235	64.3
48	SLYASSPGGVYATR	diethoxyphosphate [Y3]	P08670	vimentin	1564.7407	782.8743	67.3
49	QQYESVAAK	diethoxyphosphate [Y3]	P08670	vimentin	1159.5395	580.2736	52.0
50	SYVTTSTR	diethoxyphosphate [Y2]	P08670	vimentin	1050.4867	525.7470	51.0
51	VSGYLNLAADLAHNFTDGLAIGASFR	diethoxyphosphate [Y4]	Q92504	zinc transporter SLC39A7	2829.3971	943.8016	67.7

[a]Accession is the protein accession number in the UniProt databank [b]MH$^+$ (Da) is the calculated parent ion monoisotopic mass in charge state +1. [c]m/z (Da) is the observed monoisotopic mass divided by the charge of the parent ion. [d]% matched intensity is based on the sum of all peak heights assigned to the peptide. A matched intensity greater than 50% indicates high confidence in the assignment.

Peptides Modified on Tyrosine by Treatment with CPO

Chlorpyrifos oxon makes adducts on tyrosine, adding a mass of 136 Da to the tyrosine hydroxyl group.[14−19] Mass spectrometers have become more sensitive in the years since our first report that proteins in addition to serine hydrolases are modified by OP.[20]

Using the Orbitrap Fusion Lumos mass spectrometer, we now report OP adducts on 51 peptides from 31 proteins after treatment of human SH-SY5Y cells in serum-free medium with a nonlethal, 10 μM dose of chlorpyrifos oxon (see Table 2). Tryptic peptides had been immunopurified by binding to immobilized anti-depY monoclonal. Approximately 10% of the immunopurified peptides contained the depY modification. Labeled peptides/proteins were identified by database searches using Protein Prospector and Proteome Discoverer. Structural proteins of the cytoskeleton, including actin, tubulin, and vimentin, were diethoxyphosphorylated on several tyrosine residues. Cofilin-1, a regulator of the actin cytoskeleton, and reticulon-4, a neurite outgrowth inhibitor, were also modified on several tyrosines.

Bui-Nguyen et al. reported that dichlorvos treatment of lysed human hepatocyte-like cells resulted in modification of actin and tubulin.[21] Human neuroblastoma SH-SY5Y cells had reduced levels of f-actin following treatment with organophosphates.[22] We have no data to show that cytoskeletal identifications are statistically over-represented over random identifications. The results in Table 2 support the conclusion that the cytoskeleton is a prime target of OP toxicity.

The peptides in Table 2 had been immunopurified with monoclonal 1C6, an antibody designed to recognize diethoxyphosphorylated-tyrosine. To determine the specificity of this antibody, we also checked for diethoxyphospho adducts on serine, threonine, and lysine because these residues can be modified by OP. Candidate adducts selected by Protein Prospector and Proteome Discoverer were manually evaluated and rejected. It was concluded that monoclonal 1C6 specifically recognizes diethoxyphospho adducts on tyrosine but does not recognize diethoxyphospho adducts on serine, threonine, and lysine.

Treatment of mouse N2a cells with a nonlethal, 10 μM dose of chlorpyrifos oxon yielded 73 diethoxyphosphotyrosine-labeled peptides from 56 proteins (Table 3). Comparison of depY peptides in Tables 2 and 3 shows 10 proteins in common. The 10 proteins that are modified in both the human and mouse cells are listed in Table 4.

The cytoskeleton proteins, actin and tubulin, were modified in both human and mouse neuroblastoma cells (Table 4). Modification of cytoskeleton proteins could prevent these proteins from forming the structures necessary for neurite outgrowth. Inhibition of neurite outgrowth after exposure to 10 μM chlorpyrifos oxon has been reported.[33,34] Proteins involved in protecting the cell from stress, elongation factor 1-α 1, endoplasmin, and heat shock proteins were modified, suggesting that their function of protecting from stress may have been impaired by chlorpyrifos oxon. Mitochondrial proteins, hemoglobin and protein NipSnap homologue 3A, were modified, suggesting that chlorpyrifos oxon might adversely affect normal cell metabolism. Proteins involved in the clearance of modified proteins, proteasome subunit β type-2 and protein NipSnap homologue 3A, were modified, suggesting that clearance of damaged proteins may be disrupted, which could provide an explanation for the aggregates observed in chlorpyrifos oxon-treated N2a cells.[33]

https://doi.org/10.1021/acs.jproteome.1c00383
J. Proteome Res. 2021, 20, 4728−4745

Table 3. Diethoxyphosphate Adducts on Tyrosine in Mouse N2a Neuroblastoma Cells Treated with 10 μM Chlorpyrifos Oxon for 24 h

#	sequence	modification	accession[a]	protein	MH$^+$ (Da)[b]	m/z (Da)[c]	% matched intensity[d]
1	TIAILGAGHYVYADQPEEFNQK	diethoxyphosphate [Y10]	Q9DBL9	1-acylglycerol-3-phosphate *O*-acyltransferase ABHD5	2600.2433	867.4190	99.0
2	TIAILGAGHYVYADQPEEFNQK	diethoxyphosphate [Y12]	Q9DBL9	1-acylglycerol-3-phosphate *O*-acyltransferase ABHD5	2600.2433	867.4190	76.8
3	GYSFTTTAER	diethoxyphosphate [Y2]	P60710	actin, cytoplasmic 1	1268.5559	634.7816	78.9
4	SYELPDGQVITIGNER	diethoxyphosphate [Y2]	P60710	actin, cytoplasmic 1	1926.9209	963.9641	84.1
5	DSYVGDEAQSK	diethoxyphosphate [Y3]	P60710	actin, cytoplasmic 1 actin	1334.5512	667.7796	60.5
			P68134	α skeletal muscle			
6	AAYFGVYDTAK	diethoxyphosphate [Y7]	P48962	ADP/ATP translocase 1	1341.6137	671.3105	67.6
7	LGEYGFQNAILVR	diethoxyphosphate [Y4]	P07724	albumin	1615.8244	808.4162	81.3
8	IGAEVYHNLK	diethoxyphosphate [Y6]	P17182	α-enolase	1279.6446	427.2196	86.0
9	AAVPSGASTGIYEALELR	diethoxyphosphate [Y12]	P17182	α-enolase	1940.9747	647.6631	71.7
10	VLYNLFTK	diethoxyphosphate [Y3]	Q9EPC1	α-parvin	1133.6021	567.3047	55.0
11	GGPNYQEGLR	diethoxyphosphate [Y5]	Q3V117	ATP-citrate synthase	1226.5565	613.7818	79.6
12	YTIVVSATASDAAPLQYLAPYSGCSMGEYFR	diethoxyphosphate [Y1]	Q03265	ATP synthase subunit α, mitochondrial	3524.6132	1175.5426	68.3
13	YTIVVSATASDAAPLQYLAPYSGCSMGEYFR	diethoxyphosphate [Y17]	Q03265	ATP synthase subunit α, mitochondrial	3524.6132	1175.5426	90.3
14	ILQDYK	diethoxyphosphate [Y5]	P56480	ATP synthase subunit β, mitochondrial	915.4593	458.2333	72.2
15	AYAPGGPAYQPVVEAFGTDILHK	diethoxyphosphate [Y2]	Q9DBL7	bifunctional coenzyme A synthase	2537.2476	846.4208	93.4
16	IYWNDGLDQYR	diethoxyphosphate [Y10]	Q60967	bifunctional 3′-phospho adenosine 5′-phosphosulfate synthase 1	1578.6988	789.8530	71.6
17	LPFTPLSYIQGLSHR	diethoxyphosphate [Y8]	Q921L3	calcium load-activated calcium channel	1864.9730	622.3292	74.0
18	WQLYAAQSTK	diethoxyphosphate [Y4]	Q8VBZ3	cleft lip and palate trans membrane protein 1 homologue	1331.6395	666.3233	62.4
19	LQQLYESK	diethoxyphosphate [Y5]	Q8C9S4	coiled-coil domain-containing protein 186	1144.6113	572.8093	73.9
20	FYSVNVDYSK	diethoxyphosphate [Y2]	Q62425	cytochrome *c* oxidase subunit NDUFA4	1357.6076	679.3086	62.7
21	VTVISPGYIHTNLSVNAVTADGSR	diethoxyphosphate [Y8]	Q99J47	dehydrogenase/reductase SDR family member 7B	2607.3178	869.7773	98.3
22	FASYLTFSPSEVK	diethoxyphosphate [Y4]	Q9Z110	delta-1-pyrroline-5-carboxylate synthase	1611.7707	806.3890	68.8
23	NVSLGNVLAVAYAAK	diethoxyphosphate [Y12]	Q99KK7	dipeptidyl peptidase 3	1625.8662	813.4366	91.1
24	TGSIYWAAK	diethoxyphosphate [Y5]	P46978	dolichyl-diphosphooligo saccharide−protein glycosyl transferase subunit STT3A	1132.5438	566.7757	93.9
25	EVSTYIK	diethoxyphosphate [Y5]	P10126	elongation factor 1-α 1	975.47984	488.2437	52.5
26	EHALLAYTLGVK	diethoxyphosphate [Y7]	P10126	elongation factor 1-α 1	1450.7705	484.2614	83.2
			P62631	elongation factor 1-α 2			
27	STTTGHLIYK	diethoxyphosphate [Y9]	P10126	elongation factor 1-α 1	1256.6285	419.5477	60.6
28	DISTNYYASQK	diethoxyphosphate [Y5]	P08113	endoplasmin	1425.6298	713.3187	83.5
29	DISTNYYASQK	diethoxyphosphate [Y7]	P08113	endoplasmin	1425.6298	713.3187	83.8
30	NIYSLTPLLGQR	diethoxyphosphate [Y3]	Q9D379	epoxide hydrolase 1	1510.8029	755.9049	77.3
31	QLPYNEDSYLAR	diethoxyphosphate [Y9]	Q80UG1	fatty acid desaturase 6	1604.7357	802.8715	77.8
32	TQQHYYER	diethoxyphosphate [Y5]	Q8CI94	glycogen phosphorylase, brain	1260.5417	420.8521	57.4
33	TQQHYYER	diethoxyphosphate [Y6]	Q8CI94	glycogen phosphorylase, brain	1260.5417	420.8521	62.2
34	GYISPYFINTSK	diethoxyphosphate [Y2]	P63038	60 kDa heat shock protein, mitochondrial	1525.7353	763.3713	72.6
35	SINPDEAVAYGAAVQAAILSGDK	diethoxyphosphate [Y10]	P63017	heat shock cognate 71 kDa protein	2396.1745	799.3949	71.2
36	YESLTDPSK	diethoxyphosphate [Y1]	P07901	heat shock protein HSP 90-α	1175.5232	588.2654	51.6
			P11499	heat shock protein HSP 90-β			
37	IGGHGAEYGAEALER	diethoxyphosphate [Y8]	P01942	hemoglobin subunit α	1665.7632	555.9257	70.9
38	LLVVYPWTQR	diethoxyphosphate [Y5]	P02088	hemoglobin subunit β-1	1410.7545	705.8809	85.1

https://doi.org/10.1021/acs.jproteome.1c00383
J. Proteome Res. 2021, 20, 4728−4745

Table 3. continued

#	sequence	modification	accession[a]	protein	MH$^+$ (Da)[b]	m/z (Da)[c]	% matched intensity[d]
39	NPVWYQALTHGLNEEQR	diethoxyphosphate [Y5]	Q9EPL8	importin-7	2191.0332	731.0155	92.0
40	VTGLHQQPLCTSVNTIYDNAVQGLR	carbamidomethyl [C10]; diethoxyphosphate [Y17]	Q922Q8	leucine-rich repeat-containing protein 59	2920.4387	974.1509	80.9
41	FYGPEGPYGVFAGR	diethoxyphosphate [Y2]	O55022	membrane-associated progesterone receptor component 1	1652.7509	826.8787	61.7
42	DQEELNPYAAWR	diethoxyphosphate [Y8]	O35857	mitochondrial import inner membrane translocase subunit TIM44	1627.7152	814.3614	70.1
43	MATVYPEPQNK	diethoxyphosphate [Y5]	P06801	NADP-dependent malic enzyme	1413.6484	707.3279	87.0
44	AATADLEQYDR	diethoxyphosphate [Y9]	P81117	nucleobindin-2	1388.6094	694.8080	53.5
45	MYKEEGLNAFYK	diethoxyphosphate [Y2]	Q8VEM8	phosphate carrier protein, mitochondrial	1628.743	543.5859	65.0
46	YGYEIPVDMLCK	carbamidomethyl [C11]; diethoxyphosphate [Y1]	Q9QUM9	proteasome subunit α type-6	1623.7198	812.3637	77.1
47	YGYEIPVDMLCK	carbamidomethyl [C11]; diethoxyphosphate [Y3]	Q9QUM9	proteasome subunit α type-6	1623.7198	812.3637	73.2
48	YYTPTISR	diethoxyphosphate [Y1]	Q9R1P3	proteasome subunit β type-2	1136.5388	568.7730	58.6
49	YYTPTISR	diethoxyphosphate [Y2]	Q9R1P3	proteasome subunit β type-2	1136.5388	568.7730	55.8
50	DAYSGGAVNLYHVR	diethoxyphosphate [Y3]	O55234	proteasome subunit β type-5	1657.7734	553.2626	51.3
51	EALQLMATYLPK	diethoxyphosphate [Y9]	Q3TXS7	26S proteasome non-ATPase regulatory subunit 1	1513.7736	757.3902	92.8
52	EPYSGPTLFLLGGNSTYVQPSHHSEIR	diethoxyphosphate [Y17]	Q8K4F5	protein ABHD11	3122.4966	781.3796	80.8
53	VWYEWAVTAPVCSSIHNPTGR	carbamidomethyl [C12]; diethoxyphosphate [Y3]	Q8CIG8	protein arginine *N*-methyltransferase 5	2566.1949	856.0686	76.4
54	YTVTLGGTSFTVK	diethoxyphosphate [Y1]	Q8BGY7	protein FAM210A	1509.76	755.3835	67.8
55	TYFLKPSK	diethoxyphosphate [Y2]	Q9CQE1	protein NipSnap homologue 3B	1119.585	560.2958	76.8
56	LGQIYQSWLDK	diethoxyphosphate [Y5]	Q9CQU3	protein RER1	1486.7342	743.8709	94.5
57	LLACYK	carbamidomethyl [C4]; diethoxyphosphate [Y5]	Q9WU56	tRNA pseudouridine synthase A	903.5097	452.2585	76.4
58	AYLESEVAISEELVQK	diethoxyphosphate [Y2]	Q99P72	reticulon-4	1943.9613	648.6588	91.7
59	YSNSALGHVNSTIK	diethoxyphosphate [Y1]	Q99P72	reticulon-4	1626.7887	542.9346	50.6
60	IEGVYAR	diethoxyphosphate [Y5]	O55142	60S ribosomal protein L35a	943.4651	472.2362	89.8
61	VYDTLKGEDFLGK	diethoxyphosphate [Y2]	Q62388	serine-protein kinase ATM	1620.7921	540.9358	51.5
62	GVSAEYSFPLWK	diethoxyphosphate [Y6]	Q8BGH2	sorting and assembly machinery component 50 homologue	1519.7235	760.3654	59.1
63	GVSTVFHCASPPPYSNNK	carbamidomethyl [C8]; diethoxyphosphate [Y14]	Q9R1J0	sterol-4-α-carboxylate 3-dehydrogenase, decarboxylating	2097.9464	699.9869	93.8
64	VEYHFLSPYVSPR	diethoxyphosphate [Y3]	Q62351	transferrin receptor protein 1	1729.8362	577.2836	53.7
65	WYASLQKPSWHPPR	diethoxyphosphate [Y2]	P50637	translocator protein	1888.9258	472.9868	70.8
66	NLDIERPTYTNLNR	diethoxyphosphate [Y9]	P68369	tubulin α-1A chain	1854.911	618.9752	75.9
			P05213	tubulin α-1B chain			
67	EDAANNYAR	diethoxyphosphate [Y7]	P68369	tubulin α-1A chain	1159.4779	580.2426	73.4
			P05213	tubulin α-1B chain			
68	ISVYYNEATGGK	diethoxyphosphate [Y4]	P99024	tubulin β-5 chain	1437.6673	719.3373	73.9
69	ISVYYNEATGGK	diethoxyphosphate [Y5]	P99024	tubulin β-5 chain	1437.6673	719.3373	78.7
70	MTQNPNYYNLQGISHR	diethoxyphosphate [Y7]	Q6P4T2	U5 small nuclear ribonucleoprotein 200 kDa helicase	2071.9424	691.3190	76.2
71	MTQNPNYYNLQGISHR	diethoxyphosphate [Y8]	Q6P4T2	U5 small nuclear ribonucleoprotein 200 kDa helicase	2071.9424	691.3190	67.4
72	YQVDPDACFSAK	carbamidomethyl [C8]; diethoxyphosphate [Y1]	Q60932	voltage-dependent anion-selective channel protein 1	1536.644	768.8255	47.2

https://doi.org/10.1021/acs.jproteome.1c00383
J. Proteome Res. 2021, 20, 4728−4745

Table 3. continued

#	sequence	modification	accession[a]	protein	MH^+ (Da)[b]	m/z (Da)[c]	% matched intensity[d]
73	YQLDPTASISAK	diethoxyphosphate [Y1]	Q60930	voltage-dependent anion-selective channel protein 2	1429.6974	715.3515	51.5

[a]Accession is the protein accession number in the UniProt databank. [b]MH^+ (Da) is the calculated parent ion monoisotopic mass in charge state +1. [c]m/z (Da) is the observed monoisotopic mass divided by the charge of the parent ion. [d]% matched intensity is based on the sum of all peak heights assigned to the peptide. A matched intensity greaterthan 50% indicates high confidence in the assignment.

Table 4. Proteins Modified by 10 μM Chlorpyrifos Oxon in Both Human SH-SY5Y and Mouse N2a Cells

protein target of CPO	protein function
actin	actin cytoskeleton[23]
elongation factor 1-α 1	promotes heat shock response[24]
endoplasmin	heat shock protein 90; facilitates protein folding to active conformations[25]
heat shock proteins	ensure correct folding of stressed proteins[26]
hemoglobin	neuroprotection; maintains normal mitochondrial function[27]
proteasome subunit β type-2	proteolytic chamber for degrading damaged proteins[28]
protein NipSnap homologue 3A	mitochondrial protein induces apoptosis[29]
reticulon-4	neurite outgrowth inhibitor[30]
tubulin α	microtubule cytoskeleton[31]
tubulin β	microtubule cytoskeleton[32]

10 μM CPO Degrades to 5 μM in 24 h at 37 °C in Cell Cultures

The stability of CPO was measured in serum-free medium containing live SH-SY5Y cells at 37 °C. After 24 h, the CPO concentration dropped from 10 to 5 μM. After 5 days, the CPO concentration was 0.1 μM.

Cells Detach in 100 μM Chlorpyrifos Oxon

A 100 μM dose of chlorpyrifos oxon caused many of the mouse N2a cells in serum-free medium to detach in 24 h. The detached cells were discarded. The attached cells were collected and lysed, and the proteins were digested with trypsin. Diethoxyphosphotyrosine-containing peptides were immunopurified by binding to immobilized monoclonal 1C6 and subjected to LC-MS/MS on the Orbitrap mass spectrometer. Table S1 lists 112 peptides from 102 proteins that were found by a Proteome Discoverer database search to have been diethoxyphosphorylated on tyrosine by 100 μM CPO.

MS/MS Spectra of Cytoskeleton Peptides Immunopurified from Human SH-SY5Y Cells Treated with 10 μM Chlorpyrifos Oxon

Chlorpyrifos oxon in serum-free culture medium crossed the cell membrane and made a covalent bond with tyrosine in proteins essential for the structure of the cytoskeleton including actin, tubulin, and vimentin. MS/MS spectra in Figures 6−78 support the conclusion that actin, tubulin, and vimentin were covalently modified on tyrosine by exposure of SH-SY5Y cells to 10 μM chlorpyrifos oxon.

■ DISCUSSION

In a previous report,[7] we described a mouse monoclonal (3B9) that recognizes diethoxyphosphotyrosine peptides independent of the amino acids surrounding the modified tyrosine. The mouse monoclonal was made by hybridoma technology. The mouse monoclonal was able to immunopurify peptides modified on tyrosine by diethoxyphosphate.[14] The limitation in our 2018 study was that although adducts were detected in cell lysates treated with 1 mM chlorpyrifos oxon, we were unable to detect adducts when live cells were treated with a nonlethal dose of chlorpyrifos oxon. Our reading of the literature[35−37] and the experience of G. Xiao suggested that a rabbit monoclonal made by single B cell cloning was likely to have a higher affinity than a mouse monoclonal. The 1C6 antibody reported here fulfills this expectation. The rabbit 1C6

https://doi.org/10.1021/acs.jproteome.1c00383
J. Proteome Res. 2021, 20, 4728−4745

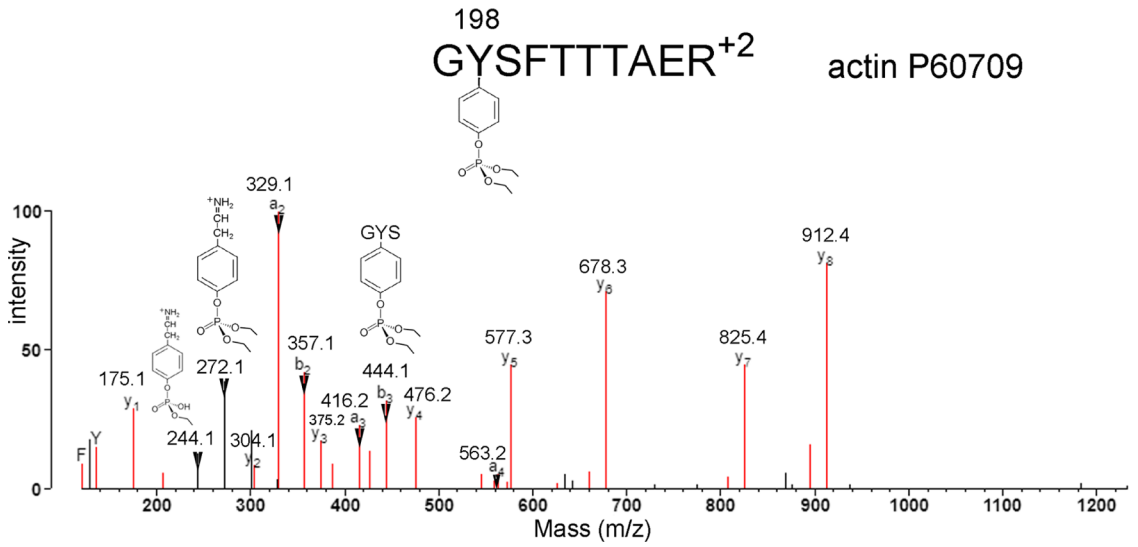

Figure 6. MS/MS spectrum of a diethoxyphosphotyrosine peptide from human actin cytoplasmic 1 (UniProt accession P60709). Seven ions marked with an arrowhead include the diethoxyphosphate mass (136.03 Da) on tyrosine: they are two immonium ions and ions a2, b2, a3, b3, and a4. The structure of the immonium ion of diethoxyphosphotyrosine is shown at 272.1 *m*/*z*. Loss of one ethylene group produces the monoethoxyphosphotyrosine immonium ion at 244.1 *m*/*z*. The structure of the b3 ion at 444.1 *m*/*z* is shown as an example of a fragment ion that includes amino acids and the adduct on tyrosine. The doubly charged parent ion has a mass of 634.7819 *m*/*z*. The diethoxyphosphate-modified residue is tyrosine 198. The y-ion series (y1−y8) supports the indicated peptide sequence.

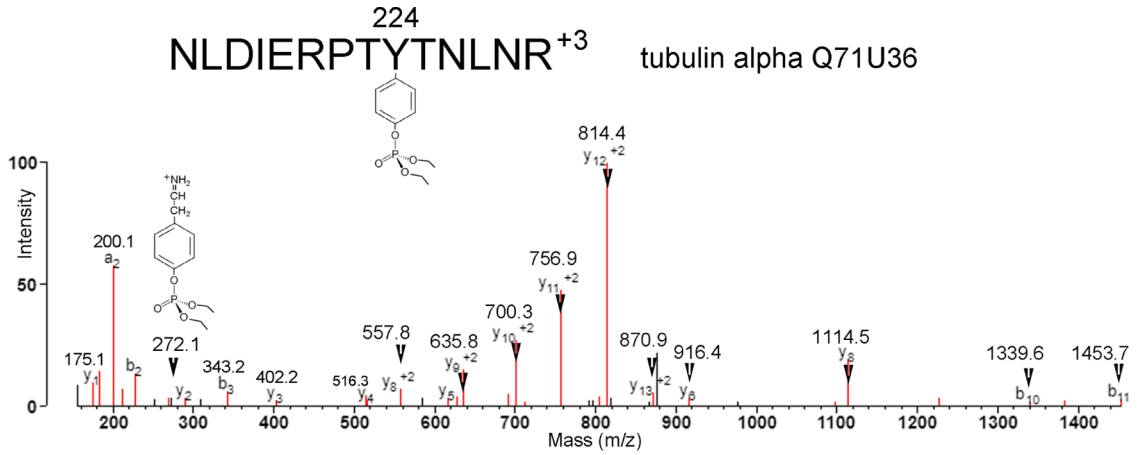

Figure 7. MS/MS spectrum of a diethoxyphosphotyrosine peptide from human tubulin α 1A chain (UniProt accession Q71U36). Eleven ions marked with an arrowhead include the diethoxyphosphate mass (136.03 Da) on tyrosine; they are the diethoxyphosphotyrosine immonium ion at 272.1 *m*/*z* and ions $y8^{+2}$, $y9^{+2}$, $y10^{+2}$, $y11^{+2}$, $y12^{+2}$, $y13^{+2}$, y6, y8, b10, and b11. The triply charged parent ion has a mass of 618.9755 *m*/*z*. The diethoxyphospho-modified residue is tyrosine 224. The y-ion series (y1−y8) and ($y8^{+2}$−$y13^{+2}$) support the indicated peptide sequence.

monoclonal has a 10-fold higher affinity for diethoxyphosphotyrosine peptides than the mouse depY monoclonal 3B9. Furthermore, the rabbit 1C6 monoclonal has a higher sensitivity for protein adducts on a Western blot. We expect the rabbit 1C6 antibody will be useful for studying mechanisms of OP toxicity.

OP can make adducts on tyrosine, lysine, threonine, and serine. We chose to make an antibody to adducts on tyrosine because diethoxyphosphate adducts on tyrosine are stable. In contrast, adducts on serine or threonine can be lost in a process called β elimination, which converts the modified serine to dehydroalanine. Adducts on lysine can undergo a spontaneous reaction with a nearby glutamic acid or aspartic acid to make an isopeptide bond with loss of the organophosphate.[38,39] The stability of OP adducts on tyrosine makes this type of adduct appropriate for studying mechanisms of OP toxicity.

Proteins Involved in OP-Induced Neurotoxicity

Evidence that proteins other than AChE are involved in OP-induced neurotoxicity comes, in part, from studies of cultured cells. The AChE inhibitors, chlorpyrifos oxon and diazoxon, interfere with differentiation of mouse N2a neuroblastoma cells by inhibiting neurite outgrowth.[33,40] Subcytotoxic concentrations of chlorpyrifos oxon reduce the levels of the neurofilament heavy-chain protein and growth-associated protein-43, two proteins important for axon outgrowth and maintenance.[33] The role of AChE in OP-induced neurotoxicity has been evaluated by treating N2a and PC12 cells with chlorpyrifos. This thiophosphate does not inhibit AChE but does inhibit the outgrowth of axon-like processes to an equal extent as chlorpyrifos oxon.[41,42] It was concluded that the neurite inhibitory effects of OP are not related to AChE inhibition.

https://doi.org/10.1021/acs.jproteome.1c00383
J. Proteome Res. 2021, 20, 4728−4745

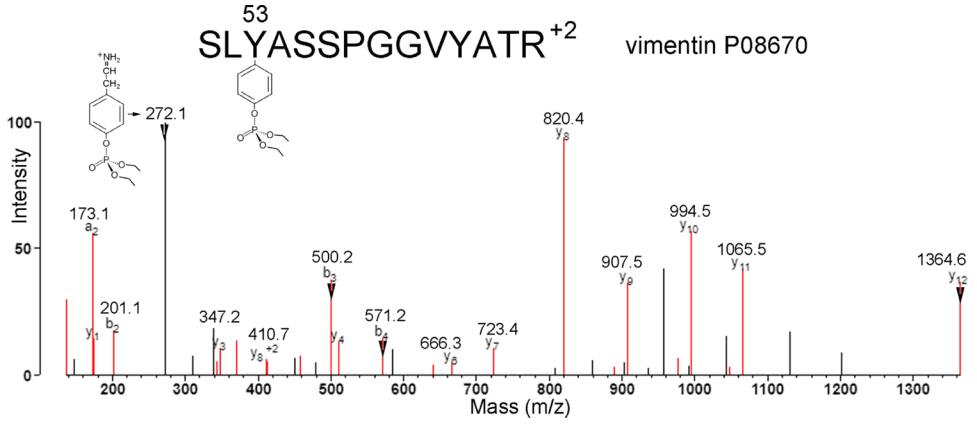

Figure 8. MS/MS spectrum of a diethoxyphosphotyrosine peptide from human vimentin (UniProt accession P08670). Four ions marked with an arrowhead include the diethoxyphosphate mass (136.03 Da) on tyrosine; they are the diethoxyphosphotyrosine immonium ion at 272.1 m/z and ions b3, b4, and y12. The doubly charged parent ion has a mass of 782.8745 m/z. The diethoxyphospho-modified residue is tyrosine 53. The y-ion series (y1−y12) supports the indicated peptide sequence.

Additional examples of OP effects independent of AChE inhibition are impaired axonal transport in a cell-free system and in rat brain,[43,44] decreased neuron synaptic spine density,[45] and hyperphosphorylation of proteins involved in axonal transport.[46−49]

Live cell imaging showed that 3 μM CPO induced the retraction of axon-like processes from predifferentiated N2a cells and that aggregates developed in cell bodies.[41] It was suggested that the OP treatment disrupted the neurofilament network. Levels of phosphorylated neurofilament heavy chain were high at 2 h after CPO treatment but declined at an 8 h exposure with no overall effect on the total level of NFH protein.[41] Results from immunoblot analyses implicated GAP-43 and MAP kinase ERK 1/2 in neurite inhibitory effects of OP.[41]

Our finding that many proteins make adducts on tyrosine following exposure to a single subcytotoxic dose of CPO raises questions. Are the OP-labeled proteins dysfunctional? How rapidly can the OP-labeled proteins be replaced by newly synthesized proteins? Does a specific OP-modified protein account for inhibition and retraction of neurite outgrowths or are the effects a consequence of many modified proteins? What percentage of a given protein is modified? Are other residues modified by OP? Do other organophosphorus pesticides and nerve agents cause similar widespread protein modifications? What is the minimal dose for OP that leads to modification in live cells or animals? What mechanism explains the long-lasting effects from low-dose exposure?

Differences between Human SH-SY5Y Neuroblastoma and Mouse N2a Neuroblastoma Cells

The number of OP-modified peptides was 73 in mouse N2a cells and 51 in human SH-SY5Y cells. Only 10 modified proteins were in common. We suggest that differences in the metabolism of these two cell lines may account for the observed difference in labeled proteins between these cell types. We find that SH-SY5Y cells grow slowly, requiring more than 6 days to reach an 80% confluence in a T75 flask. In contrast, N2a cells reach confluence overnight. SH-SY5Y cells keep a distance from other cells, whereas N2a cells grow close together. These differences are reflected in the protein concentration of cell lysates. A nearly confluent T75 flask of SH-SY5Y cells has 0.3 mg of protein in the cell lysate. A confluent T75 flask of N2a cells has 1.6 mg of protein in the cell lysate. The differences in growth rate may be the source of the differences in proteins that are susceptible to labeling by chlorpyrifos oxon.

Limitations of Monoclonal 1C6

Rabbit monoclonal 1C6 specifically recognizes diethoxyphosphate adducts on tyrosine. It does not recognize dimethoxyphosphate adducts produced by dichlorvos. Cells exposed to organophosphorus toxicants are likely to have modifications not only on tyrosine but also on lysine, threonine, and serine. Antibody 1C6 does not recognize diethoxyphosphate adducts on lysine, threonine, or serine. Antibodies to these other targets are not available in the year 2021.

New Tool to Study OP Toxicity Mechanisms

OP toxicity mechanisms independent of acetylcholinesterase inhibition could include the formation of stable, covalent adducts on tyrosine and lysine. We and others have shown that many proteins can be modified on tyrosine and lysine by OP.[14,21,50−52] Stable OP adducts could disrupt normal phosphorylation and dephosphorylation of transcription factors and regulatory proteins. This report describes a high-affinity antibody specific for diethoxyphospho adducts on tyrosine. Diethoxyphospho adducts are formed by many pesticide metabolites including chlorpyrifos oxon, diethyl paraoxon, and diazoxon. Diethoxyphospho adducts are also formed by echothiophate, an eye-drop medication for treatment of glaucoma. It is expected that the 1C6 monoclonal antibody will be useful for studies that aim to understand the long-term toxic effects of OP exposure, including the role of OP exposure in neurodegenerative diseases.

■ ASSOCIATED CONTENT

Supporting Information

The Supporting Information is available free of charge at https://pubs.acs.org/doi/10.1021/acs.jproteome.1c00383.

Diethoxyphosphotyrosine peptides in N2a cells treated with 100 μM CPO (Table S1); specificity of anti-depY monoclonal 1C6 for diethoxyphosphotyrosine-modified proteins (from CPO) (Figure S1); synthesis of diethoxyphosphotyrosine albumin; and synthesis of phosphotyrosine albumin (PDF)

https://doi.org/10.1021/acs.jproteome.1c00383
J. Proteome Res. 2021, 20, 4728−4745

AUTHOR INFORMATION

Corresponding Author

Oksana Lockridge − *Eppley Institute, University of Nebraska Medical Center, Omaha, Nebraska 68198, United States;* orcid.org/0000-0002-8345-3640; Email: olockrid@unmc.edu

Authors

Seda Onder − *Department of Biochemistry, School of Pharmacy, Hacettepe University, Ankara 06100, Turkey*

Marco van Grol − *TNO Organisation for Applied Scientific Research, 2280 AA Rijswijk, The Netherlands*

Alex Fidder − *TNO Organisation for Applied Scientific Research, 2280 AA Rijswijk, The Netherlands*

Gaoping Xiao − *Syd Labs, Inc., Hopkinton, Massachusetts 01748, United States*

Daan Noort − *TNO Organisation for Applied Scientific Research, 2280 AA Rijswijk, The Netherlands;* orcid.org/0000-0001-9267-814X

Udaya Yerramalla − *Precision Antibody, Columbia, Maryland 21045, United States*

Ozden Tacal − *Department of Biochemistry, School of Pharmacy, Hacettepe University, Ankara 06100, Turkey*

Lawrence M. Schopfer − *Eppley Institute, University of Nebraska Medical Center, Omaha, Nebraska 68198, United States;* orcid.org/0000-0002-1785-9247

Complete contact information is available at: https://pubs.acs.org/10.1021/acs.jproteome.1c00383

Author Contributions

S.O., M.v.G., A.F., G.X., and U.Y.: investigation, review, and editing; D.N. and O.T.: review and editing; L.M.S.: formal analysis, writing review, and editing; and O.L.: conceptualization, investigation, and writing the original draft.

Funding

Supported by the Fred & Pamela Buffet Cancer Center Support Grant P30CA036727, NIH grant 1R21ES030132-01A1 (to O.L.), and TUBITAK grant SBAG-318S259 (to S.O.).

Notes

The authors declare no competing financial interest.

ACKNOWLEDGMENTS

The authors thank Dr. Robert Chalkley, University of California San Francisco, for helpful advice on the use of Protein Prospector. Protein Prospector programs are available at no cost, https://prospector.ucsf.edu. Programs were developed in the University of California San Francisco Mass Spectrometry Facility, directed by Dr. Alma Burlingame, funded by the NIH National Institute for General Medical Sciences. The Proteomics Toolkit http://db.systemsbiology.net:8080/proteomicsToolkit/, Proteome Discoverer (Thermo Scientific, Waltham, MA), and XCalibur Qual Browser (Thermo Scientific, Waltham, MA) were used to identify ions in MS/MS spectra. Mass spectrometry data were obtained by the Mass Spectrometry and Proteomics Core Facility at the University of Nebraska Medical Center, which is supported by state funds from the Nebraska Research Initiative.

ABBREVIATIONS

AChE, acetylcholinesterase; BCA, bicinchoninic acid for assaying protein concentration; CPO, chlorpyrifos oxon; DMEM, Dulbecco's modified Eagle's medium; depY, diethoxyphosphate adduct on the side chain of tyrosine; ELISA, enzyme-linked immunosorbent assay; FACS, fluorescence-activated cell sorting; FBS, fetal bovine serum; GAGA, glycine, alanine, glycine, alanine; Halt protease inhibitor, AEBSF (4-(2-aminoethyl)benzenesulfonyl fluoride hydrochloride), aprotinin, bestatin, E-64, leupeptin, and pepstatin A; IP, lysis buffer immunoprecipitation buffer (25 mM Tris−HCl pH 7.4, 150 mM NaCl, 1 mM EDTA, 1% NP-40, and 5% glycerol); LC-MS/MS, liquid chromatography tandem mass spectrometry; OP, organophosphorus toxicant; Opti-MEM, reduced-serum medium; PBS, phosphate-buffered saline; pen−strep, penicillin−streptomycin; PVDF, poly(vinylidene fluoride); RIPA, buffer (20 mM Tris−HCl, pH 7.6, 150 mM NaCl, 1% NP-40, 1% sodium deoxycholate, 0.1% SDS); TBS, Tris-buffered saline (20 mM Tris−Cl, 0.15 M NaCl pH 7.5); TBST, Tris-buffered saline with 0.05% Tween-20

REFERENCES

(1) Silman, I. The multiple biological roles of the cholinesterases. *Prog. Biophys. Mol. Biol.* **2021**, *162*, 41−56.

(2) Pope, C. N. Organophosphorus pesticides: do they all have the same mechanism of toxicity? *J. Toxicol. Environ. Health, Part B* **1999**, *2*, 161−181.

(3) Sugiyama, A.; Matsuoka, T.; Sakamune, K.; Akita, T.; Makita, R.; Kimura, S.; Kuroiwa, Y.; Nagao, M.; Tanaka, J. The Tokyo subway sarin attack has long-term effects on survivors: a 10-year study started 5 years after the terrorist incident. *PLoS One* **2020**, *15*, No. e0234967.

(4) Hayden, K. M.; Norton, M. C.; Darcey, D.; Ostbye, T.; Zandi, P. P.; Breitner, J. C.; Welsh-Bohmer, K. A. Occupational exposure to pesticides increases the risk of incident AD: the Cache County study. *Neurology* **2010**, *74*, 1524−1530.

(5) Jokanović, M. Neurotoxic effects of organophosphorus pesticides and possible association with neurodegenerative diseases in man: A review. *Toxicology* **2018**, *410*, 125−131.

(6) Kamel, F.; Hoppin, J. A. Association of pesticide exposure with neurologic dysfunction and disease. *Environ. Health Perspect.* **2004**, *112*, 950−958.

(7) Onder, S.; Dafferner, A. J.; Schopfer, L. M.; Xiao, G.; Yerramalla, U.; Tacal, O.; Blake, T. A.; Johnson, R. C.; Lockridge, O. Monoclonal Antibody That Recognizes Diethoxyphosphotyrosine-Modified Proteins and Peptides Independent of Surrounding Amino Acids. *Chem. Res. Toxicol.* **2017**, *30*, 2218−2228.

(8) Schopfer, L. M.; Lockridge, O.; David, E.; Hinrichs, S. H. Purification of human butyrylcholinesterase from frozen Cohn fraction IV-4 by ion exchange and Hupresin affinity chromatography. *PLoS One* **2019**, *14*, No. e0209795.

(9) Amitai, G.; Moorad, D.; Adani, R.; Doctor, B. P. Inhibition of acetylcholinesterase and butyrylcholinesterase by chlorpyrifos-oxon. *Biochem. Pharmacol.* **1998**, *56*, 293−299.

(10) Perez-Riverol, Y.; Csordas, A.; Bai, J.; Bernal-Llinares, M.; Hewapathirana, S.; Kundu, D. J.; Inuganti, A.; Griss, J.; Mayer, G.; Eisenacher, M.; Pérez, E.; Uszkoreit, J.; Pfeuffer, J.; Sachsenberg, T.; Yilmaz, S.; Tiwary, S.; Cox, J.; Audain, E.; Walzer, M.; Jarnuczak, A. F.; Ternent, T.; Brazma, A.; Vizcaíno, J. A. The PRIDE database and related tools and resources in 2019: improving support for quantification data. *Nucleic Acids Res.* **2019**, *47*, D442−D450.

(11) Fuhs, S. R.; Meisenhelder, J.; Aslanian, A.; Ma, L.; Zagorska, A.; Stankova, M.; Binnie, A.; Al-Obeidi, F.; Mauger, J.; Lemke, G.; Yates, J. R., 3rd; Hunter, T. Monoclonal 1- and 3- phosphohistidine antibodies: new tools to study histidine phosphorylation. *Cell* **2015**, *162*, 198−210.

(12) Schopfer, L. M.; Lockridge, O. Chlorpyrifos oxon promotes tubulin aggregation via isopeptide cross-linking between diethoxyphospho-Lys and Glu or Asp: Implications for neurotoxicity. *J. Biol. Chem.* **2018**, *293*, 13566−13577.
(13) Schopfer, L. M.; Onder, S.; Lockridge, O. Evaluation of mass spectrometry MS/MS spectra for the presence of isopeptide crosslinked peptides. *PLoS One* **2021**, *16*, No. e0254450.
(14) Onder, S.; Schopfer, L. M.; Tacal, O.; Blake, T. A.; Johnson, R. C.; Lockridge, O. Mass Spectral Detection of Diethoxyphospho-Tyrosine Adducts on Proteins from HEK293 Cells Using Monoclonal Antibody depY for Enrichment. *Chem. Res. Toxicol.* **2018**, *31*, 520−530.
(15) Li, B.; Eyer, P.; Eddleston, M.; Jiang, W.; Schopfer, L. M.; Lockridge, O. Protein tyrosine adduct in humans self-poisoned by chlorpyrifos. *Toxicol. Appl. Pharmacol.* **2013**, *269*, 215−225.
(16) John, H.; Breyer, F.; Thumfart, J. O.; Hochstetter, H.; Thiermann, H. Matrix-assisted laser desorption/ionization time-of-flight mass spectrometry (MALDI-TOF MS) for detection and identification of albumin phosphylation by organophosphorus pesticides and G- and V-type nerve agents. *Anal. Bioanal. Chem.* **2010**, *398*, 2677−2691.
(17) Schopfer, L. M.; Grigoryan, H.; Li, B.; Nachon, F.; Masson, P.; Lockridge, O. Mass spectral characterization of organophosphate-labeled, tyrosine-containing peptides: characteristic mass fragments and a new binding motif for organophosphates. *J. Chromatogr. B* **2010**, *878*, 1297−1311.
(18) Grigoryan, H.; Schopfer, L. M.; Thompson, C. M.; Terry, A. V.; Masson, P.; Lockridge, O. Mass spectrometry identifies covalent binding of soman, sarin, chlorpyrifos oxon, diisopropyl fluorophosphate, and FP-biotin to tyrosines on tubulin: a potential mechanism of long term toxicity by organophosphorus agents. *Chem.-Biol. Interact.* **2008**, *175*, 180−186.
(19) van der Schans, M. J.; Hulst, A. G.; van der Riet-van Oeveren, D.; Noort, D.; Benschop, H. P.; Dishovsky, C. New tools in diagnosis and biomonitoring of intoxications with organophosphorothioates: Case studies with chlorpyrifos and diazinon. *Chem.-Biol. Interact.* **2013**, *203*, 96−102.
(20) Peeples, E. S.; Schopfer, L. M.; Duysen, E. G.; Spaulding, R.; Voelker, T.; Thompson, C. M.; Lockridge, O. Albumin, a new biomarker of organophosphorus toxicant exposure, identified by mass spectrometry. *Toxicol. Sci.* **2004**, *83*, 303−312.
(21) Bui-Nguyen, T. M.; Dennis, W. E.; Jackson, D. A.; Stallings, J. D.; Lewis, J. A. Detection of dichlorvos adducts in a hepatocyte cell line. *J. Proteome Res.* **2014**, *13*, 3583−3595.
(22) Carlson, K.; Ehrich, M. Organophosphorus compounds alter intracellular F-actin content in SH-SY5Y human neuroblastoma cells. *Neurotoxicology* **2001**, *22*, 819−827.
(23) Svitkina, T. The Actin Cytoskeleton and Actin-Based Motility. *Cold Spring Harbor Perspect. Biol.* **2018**, *10*, No. a018267.
(24) Vera, M.; Pani, B.; Griffiths, L. A.; Muchardt, C.; Abbott, C. M.; Singer, R. H.; Nudler, E. The translation elongation factor dEF1A1 couples transcription to translation during heat shock response. *eLife* **2014**, *3*, No. e03164.
(25) Zuehlke, A. D.; Moses, M. A.; Neckers, L. Heat shock protein 90: its inhibition and function. *Philos. Trans. R. Soc., B* **2018**, *373*, No. 20160527.
(26) Pratt, W. B.; Gestwicki, J. E.; Osawa, Y.; Lieberman, A. P. Targeting Hsp90/Hsp70-based protein quality control for treatment of adult onset neurodegenerative diseases. *Annu. Rev. Pharmacol. Toxicol.* **2015**, *55*, 353−371.
(27) Walser, M.; Svensson, J.; Karlsson, L.; Motalleb, R.; Aberg, M.; Kuhn, H. G.; Isgaard, J.; Aberg, N. D. Growth hormone and neuronal hemoglobin in the brain - roles in neuroprotection and neurodegenerative diseases. *Front. Endocrinol.* **2021**, *11*, No. 606089.
(28) Tomko, R. J.; Hochstrasser, M. Molecular architecture and assembly of the eukaryotic proteasome. *Annu. Rev. Biochem.* **2013**, *82*, 415−445.
(29) Fathi, E.; Yarbro, J. M.; Homayouni, R. NIPSNAP protein family emerges as a sensor of mitochondrial health. *BioEssays* **2021**, *43*, No. e2100014.
(30) Yang, Y. S.; Strittmatter, S. M. The reticulons: a family of proteins with diverse functions. *Genome Biol.* **2007**, *8*, No. 234.
(31) Eshun-Wilson, L.; Zhang, R.; Portran, D.; Nachury, M. V.; Toso, D. B.; Lohr, T.; Vendruscolo, M.; Bonomi, M.; Fraser, J. S.; Nogales, E. Effects of alpha-tubulin acetylation on microtubule structure and stability. *Proc. Natl. Acad. Sci. U.S.A.* **2019**, *116*, 10366−10371.
(32) Alushin, G. M.; Lander, G. C.; Kellogg, E. H.; Zhang, R.; Baker, D.; Nogales, E. High-resolution microtubule structures reveal the structural transitions in alphabeta-tubulin upon GTP hydrolysis. *Cell* **2014**, *157*, 1117−1129.
(33) Flaskos, J.; Nikolaidis, E.; Harris, W.; Sachana, M.; Hargreaves, A. J. Effects of sub-lethal neurite outgrowth inhibitory concentrations of chlorpyrifos oxon on cytoskeletal proteins and acetylcholinesterase in differentiating N2a cells. *Toxicol. Appl. Pharmacol.* **2011**, *256*, 330−336.
(34) Harrill, J. A.; Freudenrich, T.; Wallace, K.; Ball, K.; Shafer, T. J.; Mundy, W. R. Testing for developmental neurotoxicity using a battery of in vitro assays for key cellular events in neurodevelopment. *Toxicol. Appl. Pharmacol.* **2018**, *354*, 24−39.
(35) Rashidian, J.; Lloyd, J. Single B cell cloning and production of rabbit monoclonal antibodies. *Methods Mol. Biol.* **2020**, *2070*, 423−441.
(36) Starkie, D. O.; Compson, J. E.; Rapecki, S.; Lightwood, D. J. Generation of recombinant monoclonal antibodies from immunised mice and rabbits via flow cytometry and sorting of antigen-specific IgG+ memory B cells. *PLoS One* **2016**, *11*, No. e0152282.
(37) Seeber, S.; Ros, F.; Thorey, I.; Tiefenthaler, G.; Lifke, V.; Fischer, J. A. A.; Klostermann, S.; Endl, J.; Kopetzki, E.; Pahine, A.; Siewe, B.; Kaluza, B.; Platzer, J.; Offner, S. A robust high throughput platform to generate functional recombinant monoclonal antibodies using rabbit B cells from peripheral blood. *PLoS One* **2014**, *9*, No. e86184.
(38) Schopfer, L. M.; Lockridge, O. Mass Spectrometry Identifies Isopeptide Cross-Links Promoted by Diethylphosphorylated Lysine in Proteins Treated with Chlorpyrifos Oxon. *Chem. Res. Toxicol.* **2019**, *32*, 762−772.
(39) Schmidt, C.; Breyer, F.; Blum, M. M.; Thiermann, H.; Worek, F.; John, H. V-type nerve agents phosphonylate ubiquitin at biologically relevant lysine residues and induce intramolecular cyclization by an isopeptide bond. *Anal. Bioanal. Chem.* **2014**, *406*, 5171−5185.
(40) Sidiropoulou, E.; Sachana, M.; Flaskos, J.; Harris, W.; Hargreaves, A. J.; Woldehiwet, Z. Diazinon oxon affects the differentiation of mouse N2a neuroblastoma cells. *Arch. Toxicol.* **2009**, *83*, 373−380.
(41) Sindi, R. A.; Harris, W.; Arnott, G.; Flaskos, J.; Lloyd Mills, C.; Hargreaves, A. J. Chlorpyrifos- and chlorpyrifos oxon-induced neurite retraction in pre-differentiated N2a cells is associated with transient hyperphosphorylation of neurofilament heavy chain and ERK 1/2. *Toxicol. Appl. Pharmacol.* **2016**, *308*, 20−31.
(42) Das, K. P.; Barone, S., Jr. Neuronal differentiation in PC12 cells is inhibited by chlorpyrifos and its metabolites: is acetylcholinesterase inhibition the site of action? *Toxicol. Appl. Pharmacol.* **1999**, *160*, 217−230.
(43) Gearhart, D. A.; Sickles, D. W.; Buccafusco, J. J.; Prendergast, M. A.; Terry, A. V., Jr. Chlorpyrifos, chlorpyrifos-oxon, and diisopropylfluorophosphate inhibit kinesin-dependent microtubule motility. *Toxicol. Appl. Pharmacol.* **2007**, *218*, 20−29.
(44) Hernandez, C. M.; Beck, W. D.; Naughton, S. X.; Poddar, I.; Adam, B. L.; Yanasak, N.; Middleton, C.; Terry, A. V., Jr. Repeated exposure to chlorpyrifos leads to prolonged impairments of axonal transport in the living rodent brain. *Neurotoxicology* **2015**, *47*, 17−26.
(45) Speed, H. E.; Blaiss, C. A.; Kim, A.; Haws, M. E.; Melvin, N. R.; Jennings, M.; Eisch, A. J.; Powell, C. M. Delayed reduction of hippocampal synaptic transmission and spines following exposure to

https://doi.org/10.1021/acs.jproteome.1c00383
J. Proteome Res. 2021, 20, 4728−4745

repeated subclinical doses of organophosphorus pesticide in adult mice. *Toxicol. Sci.* **2012**, *125*, 196−208.
(46) Schuh, R. A.; Lein, P. J.; Beckles, R. A.; Jett, D. A. Noncholinesterase mechanisms of chlorpyrifos neurotoxicity: altered phosphorylation of Ca2+/cAMP response element binding protein in cultured neurons. *Toxicol. Appl. Pharmacol.* **2002**, *182*, 176−185.
(47) Gupta, R. P.; Abou-Donia, M. B. Neurofilament phosphorylation and [125I]calmodulin binding by Ca2+/calmodulin-dependent protein kinase in the brain subcellular fractions of diisopropyl phosphorofluoridate (DFP)-treated hen. *Neurochem. Res.* **1995**, *20*, 1095−1105.
(48) Gupta, R. P.; Abou-Donia, M. B. Tau phosphorylation by diisopropyl phosphorofluoridate (DFP)-treated hen brain supernatant inhibits its binding with microtubules: role of Ca2+/Calmodulin-dependent protein kinase II in tau phosphorylation. *Arch. Biochem. Biophys.* **1999**, *365*, 268−278.
(49) Choudhary, S.; Joshi, K.; Gill, K. D. Possible role of enhanced microtubule phosphorylation in dichlorvos induced delayed neurotoxicity in rat. *Brain Res.* **2001**, *897*, 60−70.
(50) Li, B.; Schopfer, L. M.; Grigoryan, H.; Thompson, C. M.; Hinrichs, S. H.; Masson, P.; Lockridge, O. Tyrosines of human and mouse transferrin covalently labeled by organophosphorus agents: a new motif for binding to proteins that have no active site serine. *Toxicol. Sci.* **2009**, *107*, 144−155.
(51) Grigoryan, H.; Li, B.; Anderson, E. K.; Xue, W.; Nachon, F.; Lockridge, O.; Schopfer, L. M. Covalent binding of the organophosphorus agent FP-biotin to tyrosine in eight proteins that have no active site serine. *Chem.-Biol. Interact.* **2009**, *180*, 492−498.
(52) Lockridge, O.; Schopfer, L. M. Review of tyrosine and lysine as new motifs for organophosphate binding to proteins that have no active site serine. *Chem.-Biol. Interact.* **2010**, *187*, 344−348.

https://doi.org/10.1021/acs.jproteome.1c00383
J. Proteome Res. 2021, 20, 4728−4745